Electronic Supplementary Material (ESI) for Dalton Transactions.

From phosphanylphosphaalkene to coordination copper and silver polymers containing P-P bond

Aleksandra Ziółkowska,[a] Marta Prześniak-Welenc,[b] Tomasz Kruczyński,[c] Michael Gamer,[d] Łukasz Ponikiewski[a*]

[a] Department of Inorganic Chemistry, Chemical Faculty, Gdansk University of Technology, Narutowicza Str. 11/12, 80-233 Gdansk, Poland;
[b] Institute of Nanotechnology and Materials Engineering, and Advanced Materials Centre, Gdansk University of Technology, Narutowicza Str. 11/12, 80-233 Gdansk, Poland;
[c] Department of Chemistry and Biochemistry, College of Science and Mathematics, Kennesaw State University, 1000 Chastain Road, Kennesaw, GA 30144, United States;
[d] Institute of Inorganic Chemistry, Karlsruhe Institute of Technology, Engesserstr. 15, 76131 Karlsruhe, Germany

PART A. NMR SPECTRA

All spectra in solution were recorded on Bruker AV400 MHz spectrometer (external standard tetramethylsilane for ^{1}H, ^{13}C; 85% H_3PO_4 for ^{31}P).

B.1. Solution NMR

B.1.1. Reaction of 1 with $HO(CH_2)_6OH$

B.1.1.2. Reaction progress of **1** with $HO(CH_2)_6OH$.

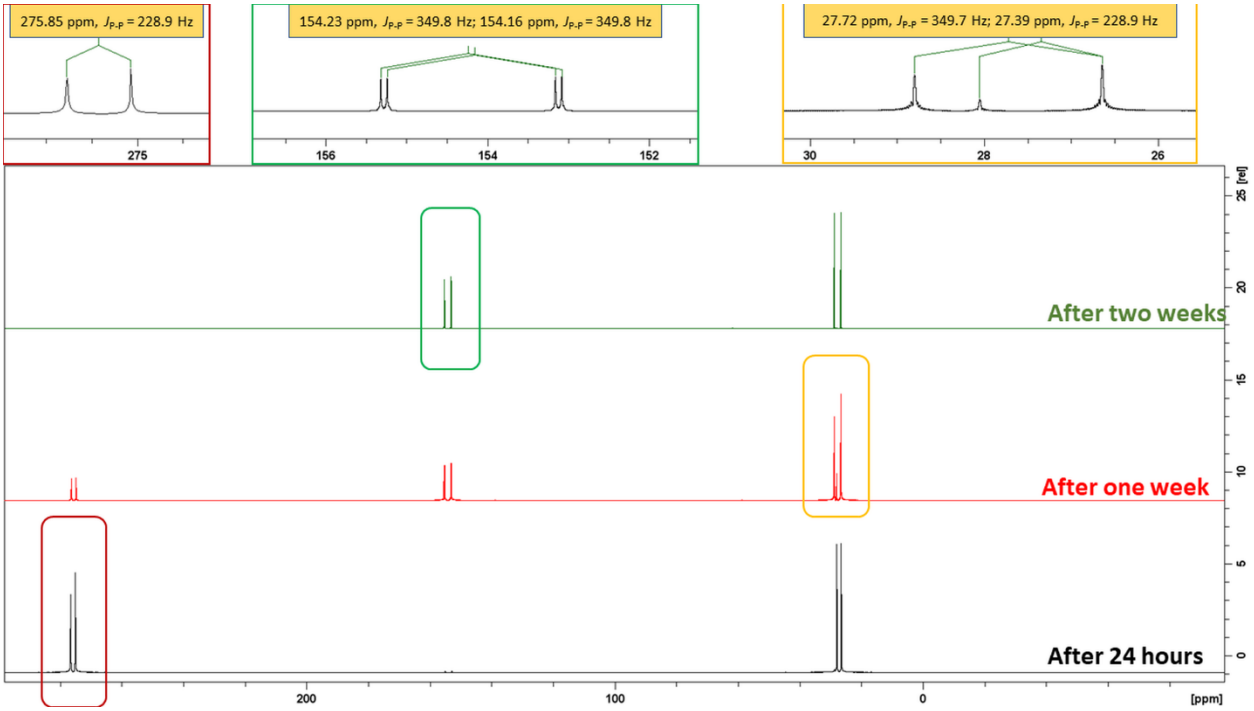

Figure S1. $^{31}P\{^{1}H\}$ NMR (THF-d_8, 400 MHz) spectra of reaction progress of **1** with $HO(CH_2)_6OH$ conducted in THF-d_8.

B.1.1.1. Spectra conducted from isolated solid residue of {(Ph)$_2$(H)C-P-P*t*Bu$_2$}{μ^2-(O-(CH$_2$)$_6$-O)}{*t*Bu$_2$P-P-C(H)(Ph)$_2$} (**2**).

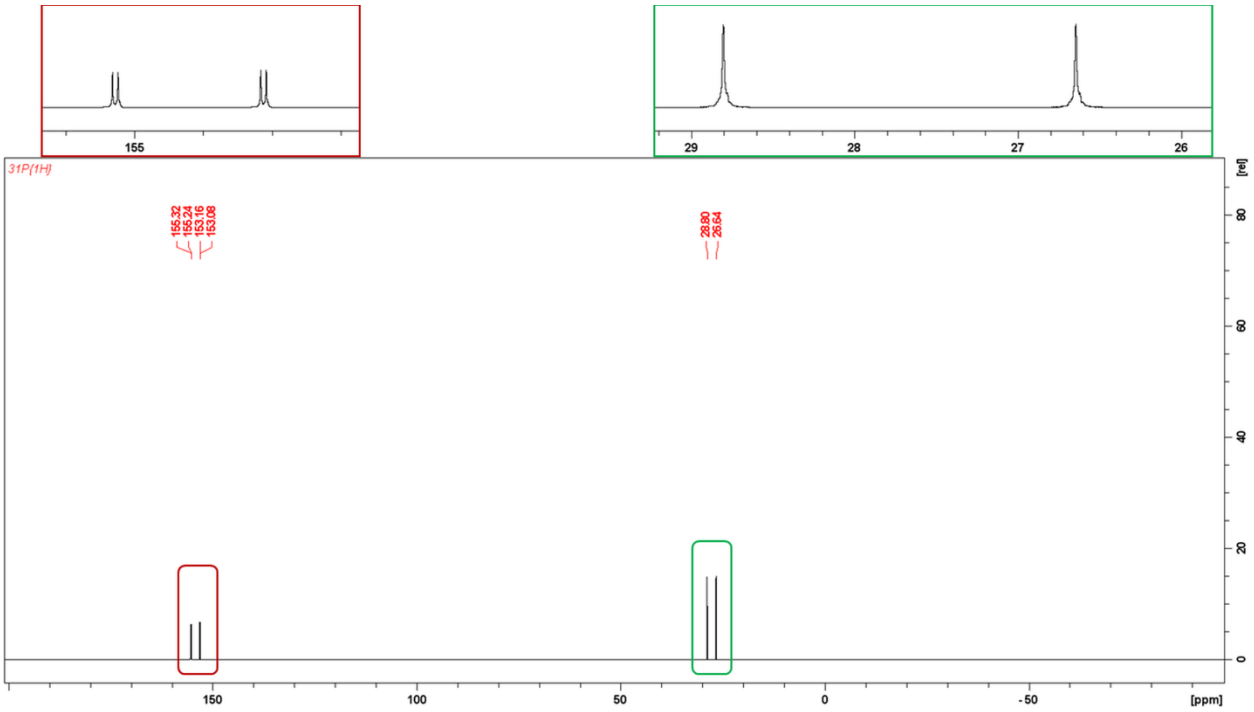

Figure S2. ^{31}P{^{1}H} NMR (THF-d$_8$, 400 MHz) spectrum of isolated with solid residue of {(Ph)$_2$(H)C-P-P*t*Bu$_2$}{μ^2-(O-(CH$_2$)$_6$-O)}{*t*Bu$_2$P-P-C(H)(Ph)$_2$} (**2**).

Mixture of two diastereomers:

- 154.23 ppm, $J_{P\text{-}P}$ = 349.8 Hz, {(Ph)$_2$(H)C-**P**-P*t*Bu$_2$}{μ^2-(O-(CH$_2$)$_6$-O)}{*t*Bu$_2$P-**P**-C(H)(Ph)$_2$};
- 154.16 ppm, $J_{P\text{-}P}$ = 349.6 Hz, {(Ph)$_2$(H)C-**P**-P*t*Bu$_2$}{μ^2-(O-(CH$_2$)$_6$-O)}{*t*Bu$_2$P-**P**-C(H)(Ph)$_2$};
- 27.72 ppm, $J_{P\text{-}P}$ = 349.7 Hz, {(Ph)$_2$(H)C-P-**P***t*Bu$_2$}{μ^2-(O-(CH$_2$)$_6$-O)}{*t*Bu$_2$**P**-P-C(H)(Ph)$_2$};

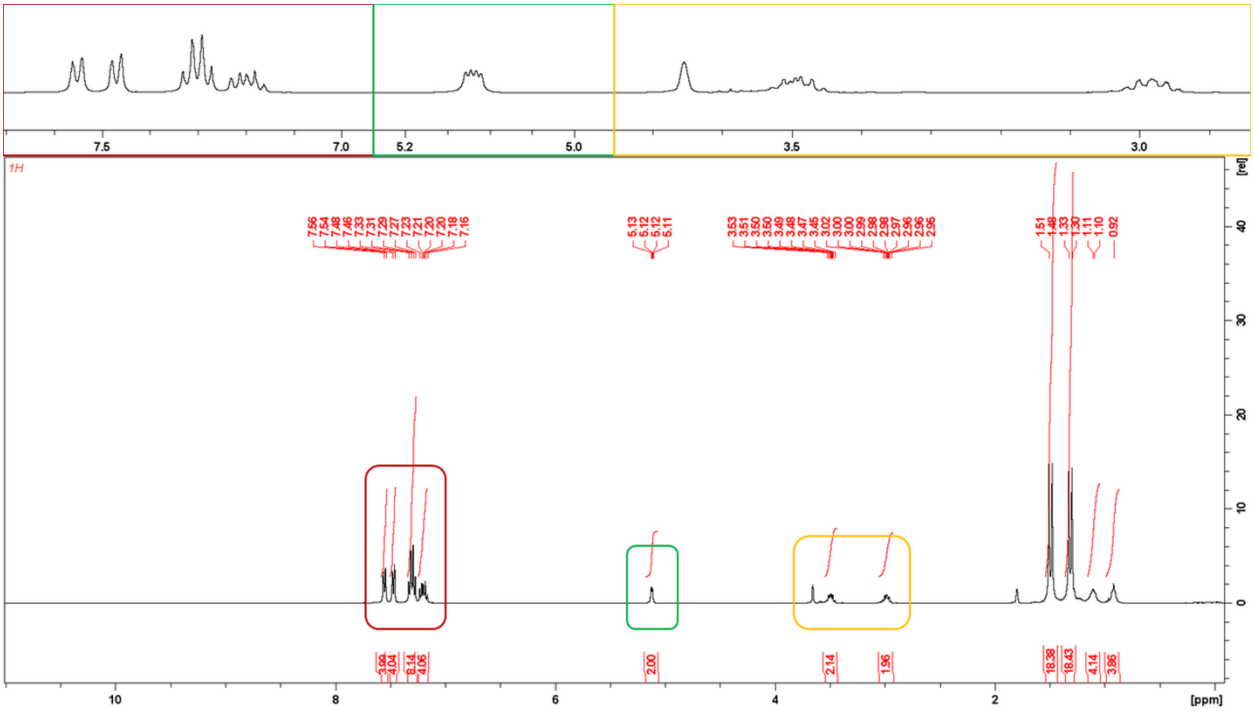

Figure S3. ^{1}H NMR (THF-d_8, 400 MHz) spectrum of isolated with solid residue of {(Ph)$_2$(H)C-P-P*t*Bu$_2$}{μ^2-(O-(CH$_2$)$_6$-O)}{*t*Bu$_2$P-P-C(H)(Ph)$_2$} (**2**).

- 7.55 ppm, broad d, 4H, $J_{H\text{-}H}$ = 8.1 Hz, {(**Ph**)$_2$(H)C-P-P*t*Bu$_2$}{μ^2-(O-(CH$_2$)$_6$-O)}{*t*Bu$_2$P-P-C(H)(**Ph**)$_2$};
- 7.47 ppm, broad d, 4H, $J_{H\text{-}H}$ = 7.7 Hz, {(**Ph**)$_2$(H)C-P-P*t*Bu$_2$}{μ^2-(O-(CH$_2$)$_6$-O)}{*t*Bu$_2$P-P-C(H)(**Ph**)$_2$};
- 7.30 ppm, broad q, 8H, $J_{H\text{-}H}$ = 16.0 Hz, $J_{H\text{-}H}$ = 7.7 Hz, {(**Ph**)$_2$(H)C-P-P*t*Bu$_2$}{μ^2-(O-(CH$_2$)$_6$-O)}{*t*Bu$_2$P-P-C(H)(**Ph**)$_2$};
- 7.20 ppm, broad m, 4H, {(**Ph**)$_2$(H)C-P-P*t*Bu$_2$}{μ^2-(O-(CH$_2$)$_6$-O)}{*t*Bu$_2$P-P-C(H)(**Ph**)$_2$};
- 5.12 ppm, dd, 2H, $J_{H\text{-}H}$ = 4.9 Hz, $J_{H\text{-}H}$ = 2.4 Hz, {(Ph)$_2$(**H**)C-P-P*t*Bu$_2$}{μ^2-(O-(CH$_2$)$_6$-O)}{*t*Bu$_2$P-P-C(**H**)(Ph)$_2$};
- 3.49 ppm, m, 2H, {(Ph)$_2$(H)C-P-P*t*Bu$_2$}{μ^2-(O-(C**H**$_2$)$_6$-O)}{*t*Bu$_2$P-P-C(H)(Ph)$_2$};
- 2.98 ppm, m, 2H, {(Ph)$_2$(H)C-P-P*t*Bu$_2$}{μ^2-(O-(C**H**$_2$)$_6$-O)}{*t*Bu$_2$P-P-C(H)(Ph)$_2$};
- 1.49 ppm, d, 18H, $J_{P\text{-}H}$ = 11.4 Hz, {(Ph)$_2$(H)C-P-P***t*Bu**$_2$}{μ^2-(O-(CH$_2$)$_6$-O)}{***t*Bu**$_2$P-P-C(H)(Ph)$_2$};
- 1.31 ppm, d, 18H, $J_{P\text{-}H}$ = 11.6 Hz, {(Ph)$_2$(H)C-P-P***t*Bu**$_2$}{μ^2-(O-(CH$_2$)$_6$-O)}{***t*Bu**$_2$P-P-C(H)(Ph)$_2$};
- 1.10 ppm, broad m, 4H, {(Ph)$_2$(H)C-P-P*t*Bu$_2$}{μ^2-(O-(C**H**$_2$)$_6$-O)}{*t*Bu$_2$P-P-C(H)(Ph)$_2$};
- 0.92 ppm, broad m, 4H, {(Ph)$_2$(H)C-P-P*t*Bu$_2$}{μ^2-(O-(C**H**$_2$)$_6$-O)}{*t*Bu$_2$P-P-C(H)(Ph)$_2$};

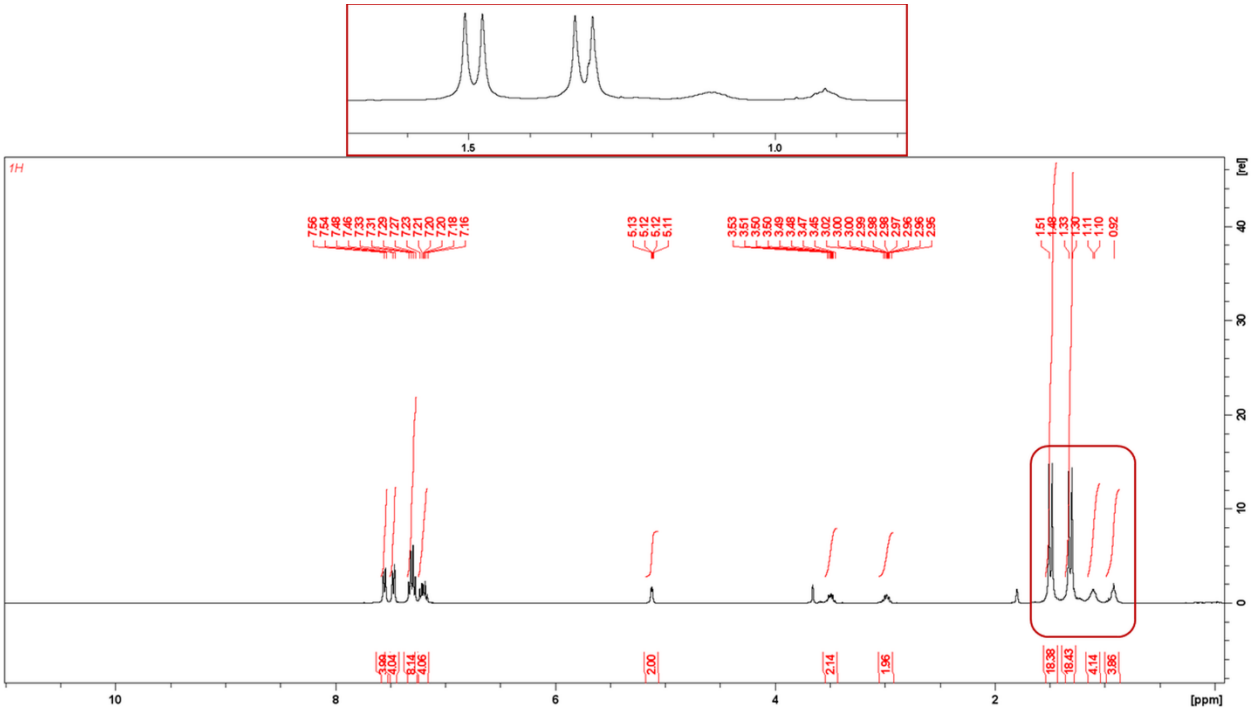

Figure S4. ^{1}H NMR (THF-d_8, 400 MHz) spectrum of isolated with solid residue of {$(Ph)_2$(H)C-P-P*t*Bu_2}{μ^2-(O-$(CH_2)_6$-O)}{*t*Bu_2P-P-C(H)$(Ph)_2$} (**2**).

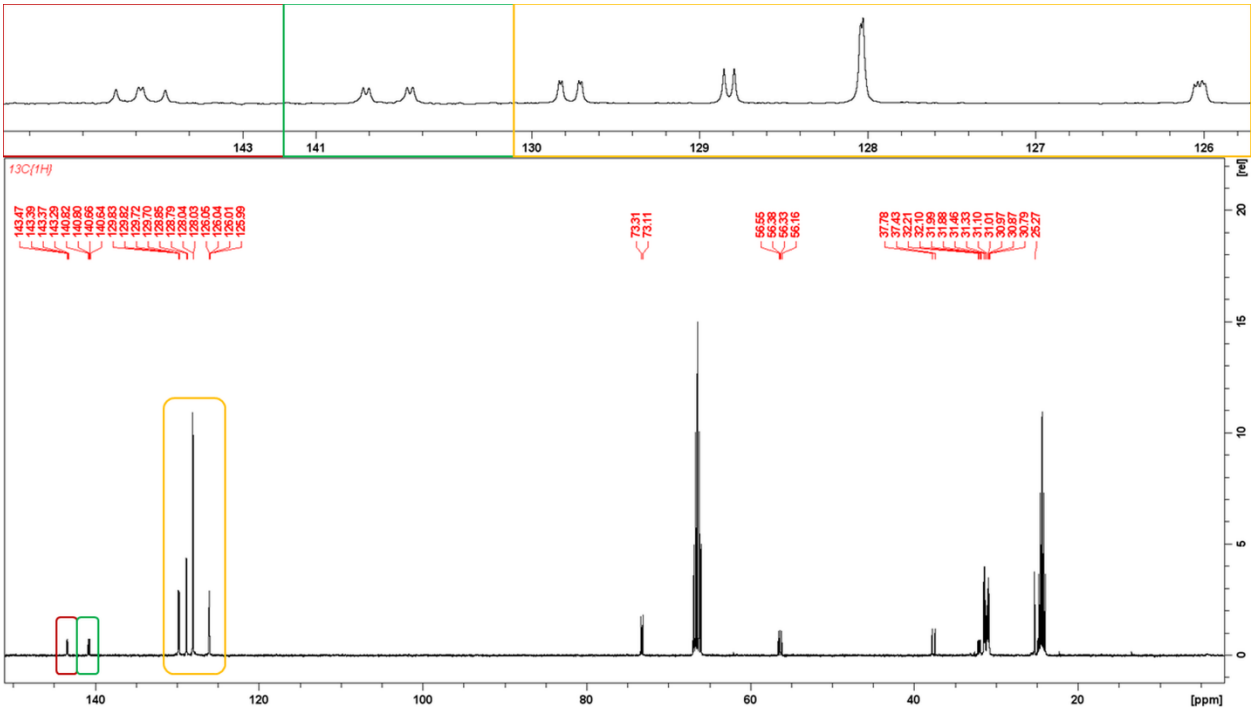

Figure S5. $^{13}C\{^{1}H\}$ NMR (THF-d_8, 400 MHz) spectrum of isolated with solid residue of {$(Ph)_2$(H)C-P-P*t*Bu_2}{μ^2-(O-$(CH_2)_6$-O)}{*t*Bu_2P-P-C(H)$(Ph)_2$} (**2**).

Aromatic carbon atoms:

- 143.38 ppm, dd, $J_{P\text{-}C}$ = 10.1 Hz, $J_{P\text{-}C}$ = 8.5 Hz;
- 140.73 ppm, dd, $J_{P\text{-}C}$ = 16.5 Hz, $J_{P\text{-}C}$ = 2.1 Hz;
- 129.76 ppm, dd, $J_{P\text{-}C}$ = 11.7 Hz, $J_{P\text{-}C}$ = 1.6 Hz;
- 128.82 ppm, d, $J_{P\text{-}C}$ = 6.3 Hz;
- 128.03 ppm, d, $J_{P\text{-}C}$ = 1.4 Hz;
- 126.02 ppm, dd, $J_{P\text{-}C}$ = 4.4 Hz, $J_{P\text{-}C}$ = 2.0 Hz;

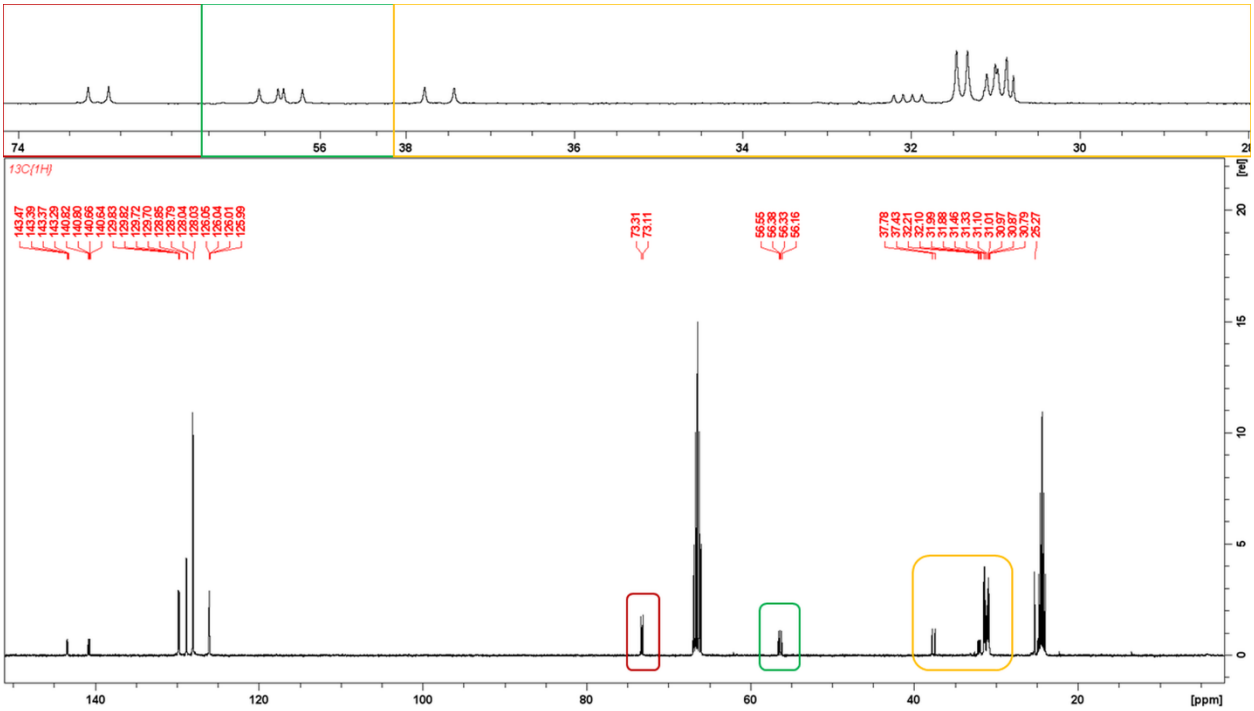

Figure S6. $^{13}C\{^{1}H\}$ NMR (THF-d_8, 400 MHz) spectrum of isolated with solid residue of $\{(Ph)_2(H)C\text{-}P\text{-}PtBu_2\}\{\mu^2\text{-}(O\text{-}(CH_2)_6\text{-}O)\}\{tBu_2P\text{-}P\text{-}C(H)(Ph)_2\}$ (**2**).

- 73.21 ppm, d, $J_{P\text{-}C}$ = 20.3 Hz, $\{(Ph)_2(H)C\text{-}P\text{-}PtBu_2\}\{\mu^2\text{-}(O\text{-}(\mathbf{C}H_2)_6\text{-}O)\}\{tBu_2P\text{-}P\text{-}C(H)(Ph)_2\}$;
- 56.35 ppm, dd, $J_{P\text{-}C}$ = 21.9 Hz, $J_{P\text{-}C}$ = 16.9 Hz; $\{(Ph)_2(H)\mathbf{C}\text{-}P\text{-}PtBu_2\}\{\mu^2\text{-}(O\text{-}(CH_2)_6\text{-}O)\}\{tBu_2P\text{-}P\text{-}\mathbf{C}(H)(Ph)_2\}$;
- 37.60 ppm, d, $J_{P\text{-}C}$ = 35.3 Hz, $\{(Ph)_2(H)C\text{-}P\text{-}P\{\mathbf{C}(CH_3)_3\}_2\}\{\mu^2\text{-}(O\text{-}(CH_2)_6\text{-}O)\}\{\{(H_3C)_3\mathbf{C}\}_2P\text{-}P\text{-}C(H)(Ph)_2\}$;
- 32.04 ppm, dd, $J_{P\text{-}C}$ = 22.2 Hz, $J_{P\text{-}C}$ = 11.3 Hz, $\{(Ph)_2(H)C\text{-}P\text{-}P\{\mathbf{C}(CH_3)_3\}_2\}\{\mu^2\text{-}(O\text{-}(CH_2)_6\text{-}O)\}\{\{(H_3C)_3\mathbf{C}\}_2P\text{-}P\text{-}C(H)(Ph)_2\}$;
- 31.40 ppm, d, $J_{P\text{-}C}$ = 13.2 Hz, $\{(Ph)_2(H)C\text{-}P\text{-}P\{C(\mathbf{C}H_3)_3\}_2\}\{\mu^2\text{-}(O\text{-}(CH_2)_6\text{-}O)\}\{\{(H_3\mathbf{C})_3C\}_2P\text{-}P\text{-}C(H)(Ph)_2\}$;
- 30.98 ppm, d, $J_{P\text{-}C}$ = 10.2 Hz, $\{(Ph)_2(H)C\text{-}P\text{-}P\{C(\mathbf{C}H_3)_3\}_2\}\{\mu^2\text{-}(O\text{-}(CH_2)_6\text{-}O)\}\{\{(H_3\mathbf{C})_3C\}_2P\text{-}P\text{-}C(H)(Ph)_2\}$;
- 30.83 ppm, d, $J_{P\text{-}C}$ = 8.2 Hz, $\{(Ph)_2(H)C\text{-}P\text{-}PtBu_2\}\{\mu^2\text{-}(O\text{-}(\mathbf{C}H_2)_6\text{-}O)\}\{tBu_2P\text{-}P\text{-}C(H)(Ph)_2\}$;
- 30.83 ppm, d, $J_{P\text{-}C}$ = 8.2 Hz, $\{(Ph)_2(H)C\text{-}P\text{-}PtBu_2\}\{\mu^2\text{-}(O\text{-}(\mathbf{C}H_2)_6\text{-}O)\}\{tBu_2P\text{-}P\text{-}C(H)(Ph)_2\}$;
- 25.27 ppm, s, $\{(Ph)_2(H)C\text{-}P\text{-}PtBu_2\}\{\mu^2\text{-}(O\text{-}(\mathbf{C}H_2)_6\text{-}O)\}\{tBu_2P\text{-}P\text{-}C(H)(Ph)_2\}$;

B.1.1.3. Spectra conducted from reaction mixture after reaction of **1** with $HO(CH_2)_6OH$ in the presence of *t*BuOK as catalyst (10% molar).

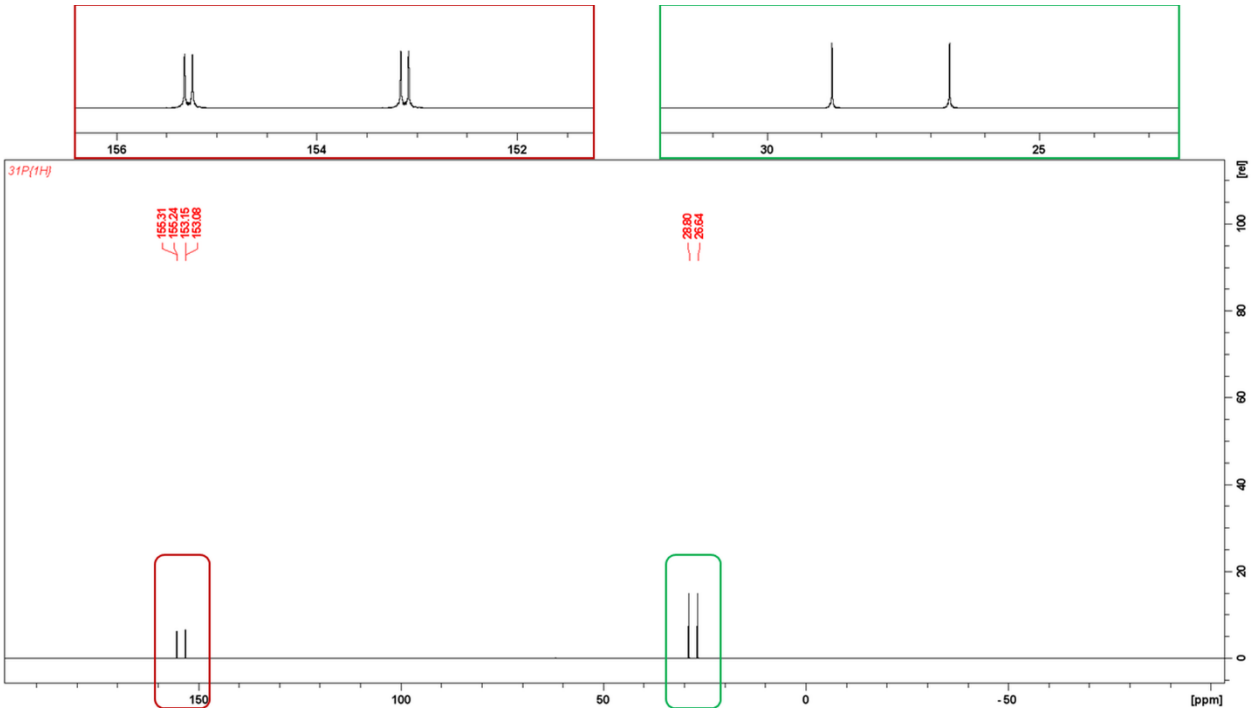

Figure S7. $^{31}P\{^{1}H\}$ NMR (THF-d_8, 400 MHz) spectra of reaction mixture of **1** with $HO(CH_2)_6OH$ in the presence of *t*BuOK as catalyst (10% molar) conducted in THF-d_8.

- 154.23 ppm, $J_{P\text{-}P}$ = 349.8 Hz, $\{(Ph)_2(H)C\text{-}\mathbf{P}\text{-}P t Bu_2\}\{\mu^2\text{-}(O\text{-}(CH_2)_6\text{-}O)\}\{t Bu_2P\text{-}\mathbf{P}\text{-}C(H)(Ph)_2\}$;
- 154.16 ppm, $J_{P\text{-}P}$ = 349.6 Hz, $\{(Ph)_2(H)C\text{-}\mathbf{P}\text{-}P t Bu_2\}\{\mu^2\text{-}(O\text{-}(CH_2)_6\text{-}O)\}\{t Bu_2P\text{-}\mathbf{P}\text{-}C(H)(Ph)_2\}$;
- 27.72 ppm, $J_{P\text{-}P}$ = 349.7 Hz, $\{(Ph)_2(H)C\text{-}P\text{-}\mathbf{P}t Bu_2\}\{\mu^2\text{-}(O\text{-}(CH_2)_6\text{-}O)\}\{t Bu_2\mathbf{P}\text{-}P\text{-}C(H)(Ph)_2\}$;

B.1.2. Reaction of 1 with $HS(CH_2)_4SH$

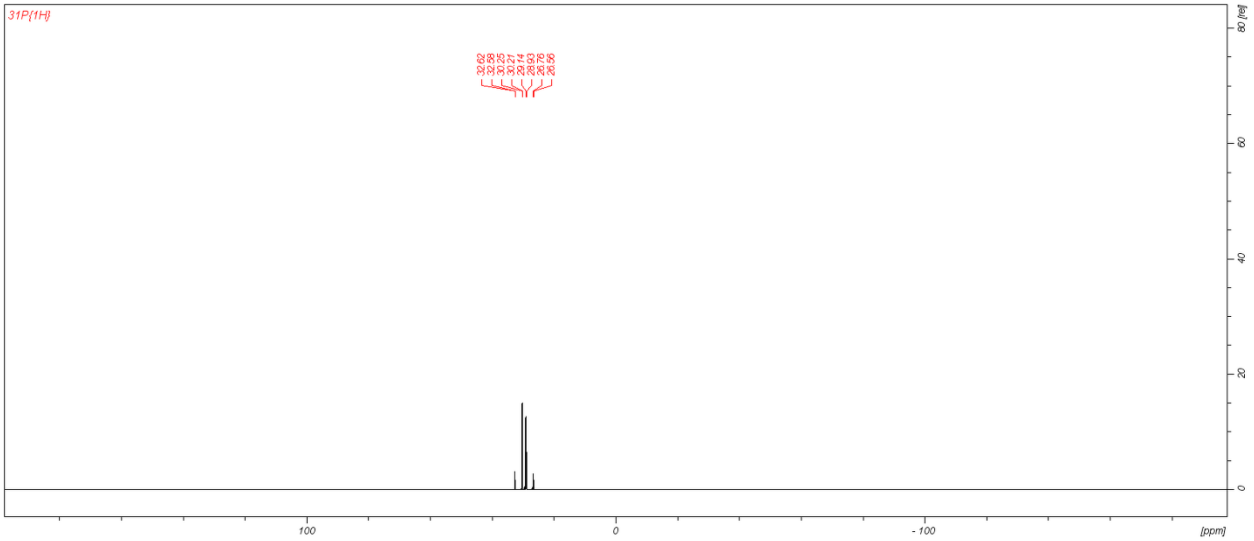

Figure S8. $^{31}P\{^{1}H\}$ NMR (C_6D_6, 162 MHz) spectrum of isolated crystals of $\{(Ph)_2(H)C\text{-}P\text{-}PtBu_2\}\{\mu^2\text{-}(S\text{-}(CH_2)_4\text{-}S)\}\{tBu_2P\text{-}P\text{-}C(H)(Ph)_2\}$ (**3a**).

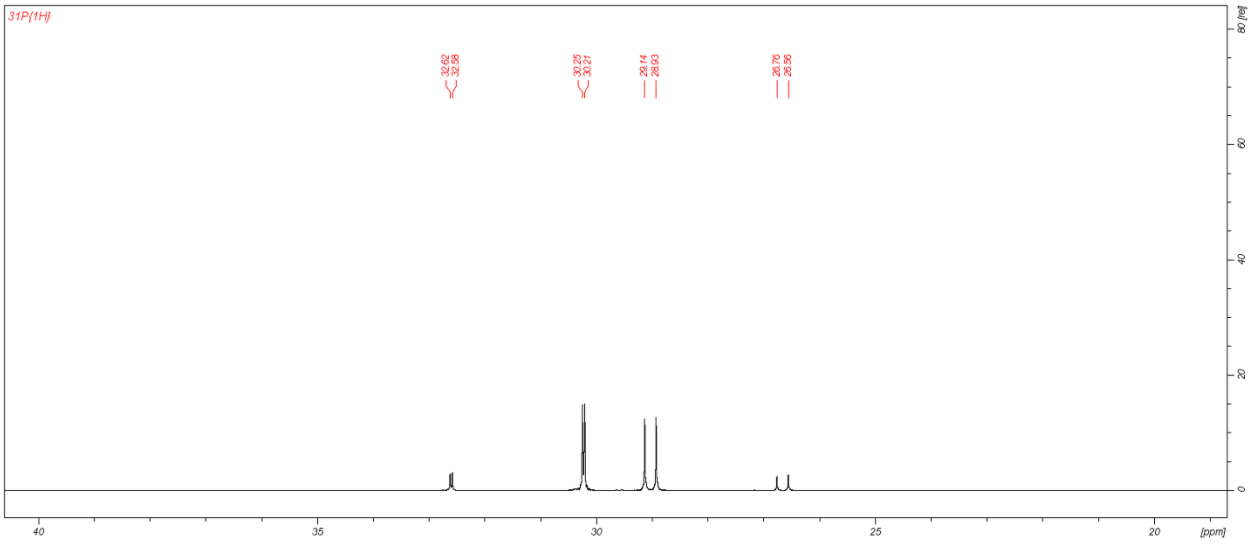

Figure S9. $^{31}P\{^{1}H\}$ NMR (C_6D_6, 162 MHz) spectrum of isolated crystals of {$(Ph)_2$(H)C-P-P*t*Bu_2}{μ^2-(S-$(CH_2)_4$-S)}{*t*Bu_2P-P-C(H)$(Ph)_2$} (**3a**) in narrow range from 40 ppm to 20 ppm.

Mixture of two diastereomers:

- 31.44 ppm, d, $J_{P\text{-}P}$ = 384.2 Hz, {$(Ph)_2$(H)C-P-**P***t*Bu_2}{μ^2-(S-$(CH_2)_4$-S)}{*t*Bu_2**P**-P-C(H)$(Ph)_2$};
- 27.75 ppm, d, $J_{P\text{-}P}$ = 384.2 Hz, {$(Ph)_2$(H)C-**P**-P*t*Bu_2}{μ^2-(S-$(CH_2)_4$-S)}{*t*Bu_2P-**P**-C(H)$(Ph)_2$};
- 31.40 ppm, d, $J_{P\text{-}P}$ = 384.2 Hz, {$(Ph)_2$(H)C-P-**P***t*Bu_2}{μ^2-(S-$(CH_2)_4$-S)}{*t*Bu_2**P**-P-C(H)$(Ph)_2$};
- 27.95 ppm, d, $J_{P\text{-}P}$ = 384.2 Hz, {$(Ph)_2$(H)C-**P**-P*t*Bu_2}{μ^2-(S-$(CH_2)_4$-S)}{*t*Bu_2P-**P**-C(H)$(Ph)_2$};

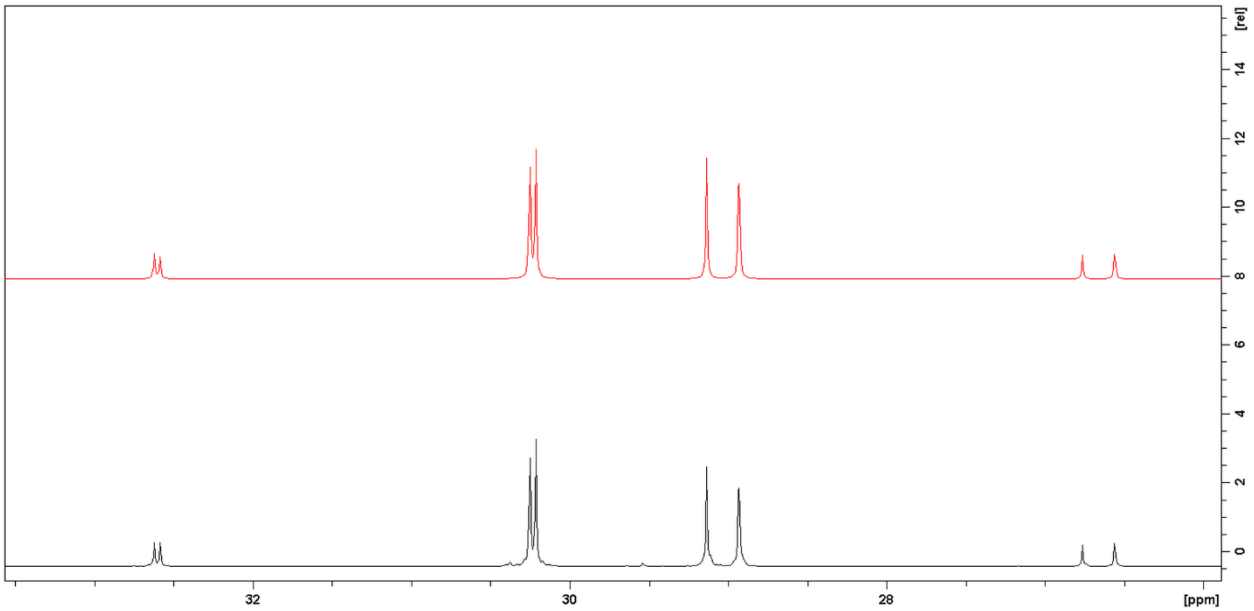

Figure S10. $^{31}P\{^{1}H\}$ NMR (C_6D_6, 162 MHz) spectrum of isolated crystals of **3a** – black color;

$^{31}P\{^{1}H\}$ NMR simulation spectrum of **3a** – red color;

Mixture of two diastereomers; Simulation parameters:

Statistical weight: 1.0000

- 30.96 ppm, d, $J_{P\text{-}P}$ = 384.1 Hz;
- 28.18 ppm, d, $J_{P\text{-}P}$ = 384.1 Hz;

Statistical weight: 0.9987

- 30.97 ppm, d, $J_{P\text{-}P}$ = 384.2 Hz;
- 28.41 ppm, d, $J_{P\text{-}P}$ = 384.2 Hz;

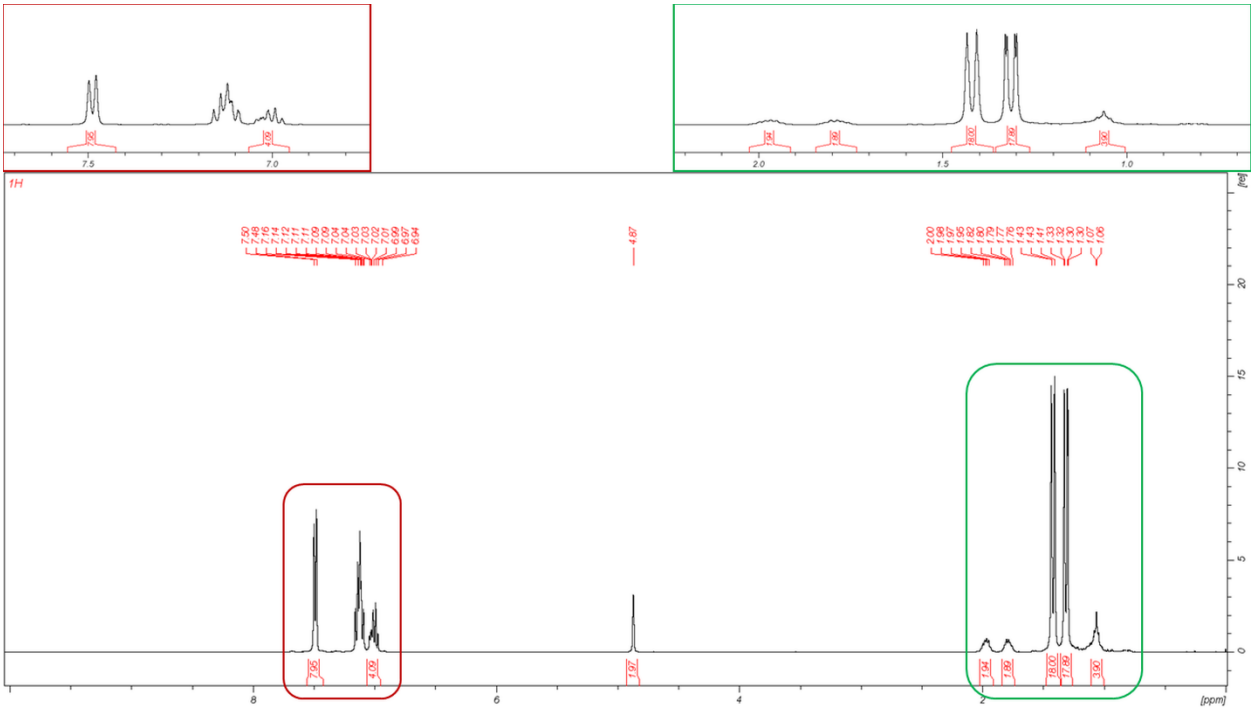

Figure S11. ^{1}H NMR (C_6D_6, 400 MHz) spectrum of isolated crystals of {(Ph)$_2$(H)C-P-P*t*Bu$_2$}{μ^2-(S-(CH$_2$)$_4$-S)}{*t*Bu$_2$P-P-C(H)(Ph)$_2$} (**3a**).

- 7.50 – 6.94 ppm, aromatic protons, 20H, {(**Ph**)$_2$(H)C-P-P*t*Bu$_2$}{μ^2-(S-(CH$_2$)$_4$-S)}{*t*Bu$_2$P-P-C(H)(**Ph**)$_2$};
- 4.87 ppm, s, 2H, {(Ph)$_2$(**H**)C-P-P*t*Bu$_2$}{μ^2-(S-(CH$_2$)$_4$-S)}{*t*Bu$_2$P-P-C(**H**)(Ph)$_2$};
- 1.97 ppm, broad m, 2H, {(Ph)$_2$(H)C-P-P*t*Bu$_2$}{μ^2-(S-(C**H**$_2$)$_4$-S)}{*t*Bu$_2$P-P-C(H)(Ph)$_2$};
- 1.79 ppm, broad m, 2H, {(Ph)$_2$(H)C-P-P*t*Bu$_2$}{μ^2-(S-(C**H**$_2$)$_4$-S)}{*t*Bu$_2$P-P-C(H)(Ph)$_2$};
- 1.42 ppm, broad d, $J_{P\text{-}H}$ = 10.5 Hz, 18H, {(Ph)$_2$(H)C-P-P***t*****Bu**$_2$}{μ^2-(S-(CH$_2$)$_4$-S)}{***t*****Bu**$_2$P-P-C(H)(Ph)$_2$};
- 1.31 ppm, dd, $J_{P\text{-}H}$ = 10.44 Hz, $J_{P\text{-}H}$ = 2.1 Hz, 18H, {(Ph)$_2$(H)C-P-P***t*****Bu**$_2$}{μ^2-(S-(CH$_2$)$_4$-S)}{***t*****Bu**$_2$P-P-C(H)(Ph)$_2$};
- 1.07 ppm, broad m, 4H, {(Ph)$_2$(H)C-P-P*t*Bu$_2$}{μ^2-(S-(C**H**$_2$)$_4$-S)}{*t*Bu$_2$P-P-C(H)(Ph)$_2$};

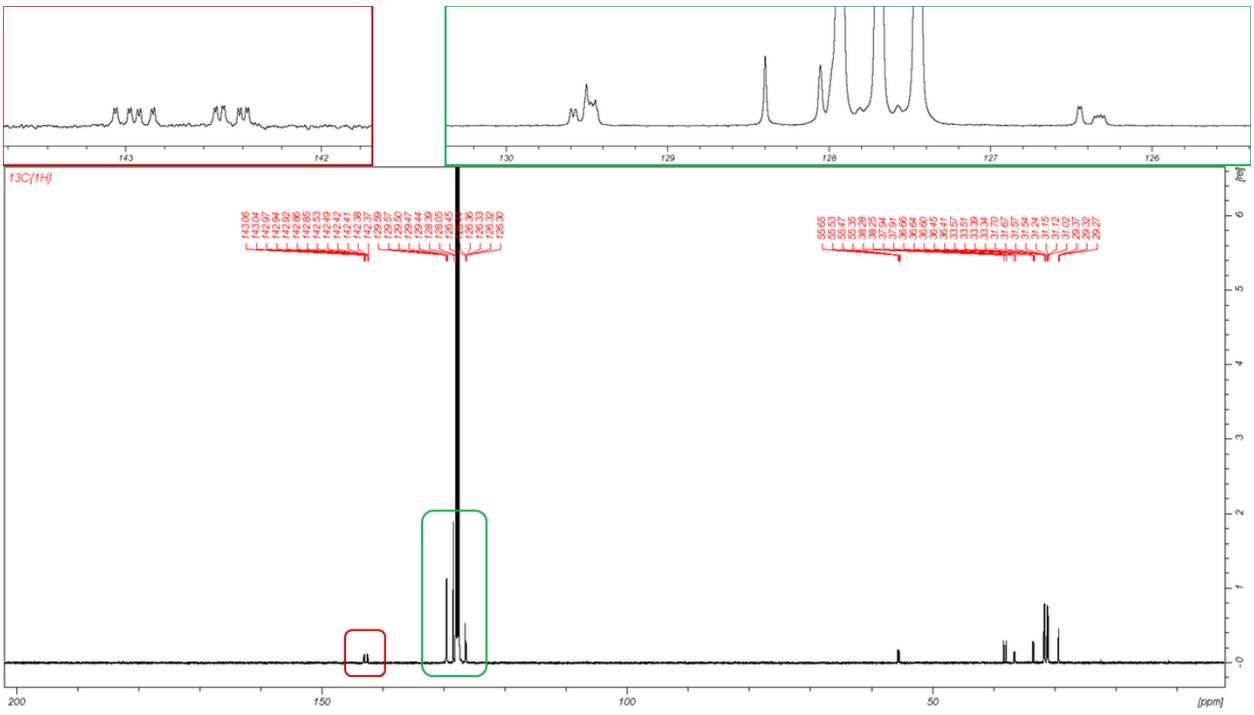

Figure S12. $^{13}C\{^{1}H\}$ NMR (C_6D_6, 100.62 MHz) spectrum of isolated crystals of {$(Ph)_2$(H)C-P-P*t*Bu_2}{μ^2-(S-$(CH_2)_4$-S)}{*t*Bu_2P-P-C(H)$(Ph)_2$} (**3a**).

Aromatic carbon atoms:

- 142.95 ppm, ddd, $J_{P\text{-}C}$ = 12.1 Hz, $J_{P\text{-}C}$ = 7.3 Hz, $J_{P\text{-}C}$ = 1.3 Hz;
- 142.46 ppm, ddd, $J_{P\text{-}C}$ = 12.4 Hz, $J_{P\text{-}C}$ = 3.8 Hz, $J_{P\text{-}C}$ = 1.2 Hz;
- 129.58 ppm, d, $J_{P\text{-}C}$ = 2.7 Hz;
- 129.50 ppm, s;
- 129.46 ppm, d, $J_{P\text{-}C}$ = 2.8 Hz;
- 128.39 ppm, s;
- 128.05 ppm, s;
- 126.45 ppm, d, $J_{P\text{-}C}$ = 1.7 Hz;
- 126.33 ppm, dd, $J_{P\text{-}C}$ = 4.2 Hz, $J_{P\text{-}C}$ = 2.1 Hz;

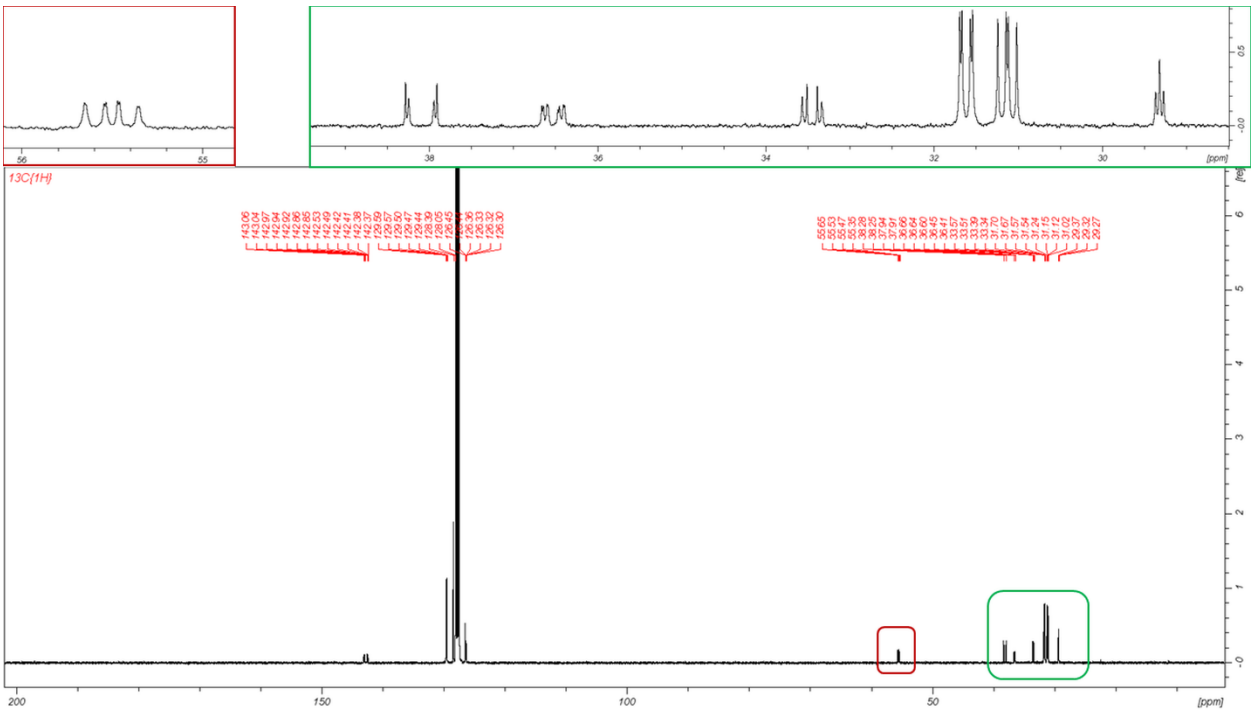

Figure S13. $^{13}C\{^{1}H\}$ NMR (C_6D_6, 100.62 MHz) spectrum of isolated crystals of {$(Ph)_2$(H)C-P-P*t*Bu_2}{μ^2-(S-$(CH_2)_4$-S)}{*t*Bu_2P-P-C(H)$(Ph)_2$} (**3a**).

- 55.50 ppm, ddd, $J_{P\text{-}C}$ = 18.6 Hz, $J_{P\text{-}C}$ = 11.0 Hz, $J_{P\text{-}C}$ = 1.1 Hz, {$(Ph)_2$(H)**C**-P-P{$C(CH_3)_3$}$_2$}{μ^2-(S-$(CH_2)_4$-S)}{{$(H_3C)_3$C}$_2$P-P-**C**(H)$(Ph)_2$};
- 38.10 ppm, dd, $J_{P\text{-}C}$ = 34.1 Hz, $J_{P\text{-}C}$ = 3.5 Hz, {$(Ph)_2$(H)C-P-P{$C(CH_3)_3$}$_2$}{μ^2-(S-(**C**H_2)$_4$-S)}{{$(H_3C)_3$C}$_2$P-P-C(H)$(Ph)_2$}.
- 36.53 ppm, ddd, $J_{P\text{-}C}$ = 19.2 Hz, $J_{P\text{-}C}$ = 6.1 Hz, $J_{P\text{-}C}$ = 1.9 Hz, {$(Ph)_2$(H)C-P-P{**C**$(CH_3)_3$}$_2$}{μ^2-(S-$(CH_2)_4$-S)}{{$(H_3C)_3$**C**}$_2$P-P-C(H)$(Ph)_2$};
- 33.45 ppm, dd, $J_{P\text{-}C}$ = 18.2 Hz, $J_{P\text{-}C}$ = 5.7 Hz, {$(Ph)_2$(H)C-P-P{**C**$(CH_3)_3$}$_2$}{μ^2-(S-$(CH_2)_4$-S)}{{$(H_3C)_3$**C**}$_2$P-P-C(H)$(Ph)_2$};
- 31.62 ppm, dd, $J_{P\text{-}C}$ = 12.6 Hz, $J_{P\text{-}C}$ = 2.7 Hz, {$(Ph)_2$(H)C-P-P{C(**C**$H_3)_3$}$_2$}{μ^2-(S-$(CH_2)_4$-S)}{{$(H_3$**C**$)_3$C}$_2$P-P-C(H)$(Ph)_2$};
- 31.13 ppm, dd, $J_{P\text{-}C}$ = 12.8 Hz, $J_{P\text{-}C}$ = 9.9 Hz, {$(Ph)_2$(H)C-P-P{C(**C**$H_3)_3$}$_2$}{μ^2-(S-$(CH_2)_4$-S)}{{$(H_3$**C**$)_3$C}$_2$P-P-C(H)$(Ph)_2$};
- 29.35 ppm, t, $J_{P\text{-}C}$ = 5.0 Hz, {$(Ph)_2$(H)C-P-P*t*Bu_2}{μ^2-(S-(**C**H_2)$_4$-S)}{*t*Bu_2P-P-C(H)$(Ph)_2$};

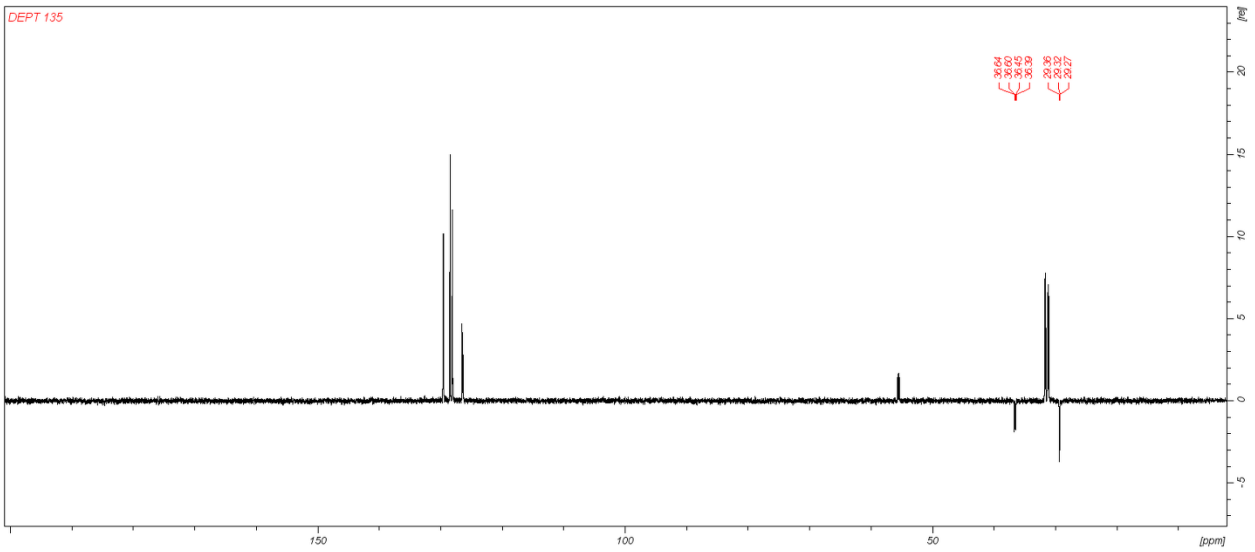

Figure S14. $^{13}C\{^{1}H\}$ NMR-dept135 (C_6D_6, 100.62 MHz) spectrum of isolated crystals of $\{(Ph)_2(H)C\text{-}P\text{-}PtBu_2\}\{\mu^2\text{-}(S\text{-}(CH_2)_4\text{-}S)\}\{tBu_2P\text{-}P\text{-}C(H)(Ph)_2\}$ (**3a**).

B.1.3. Reaction of 1 with HSC_6H_4SH

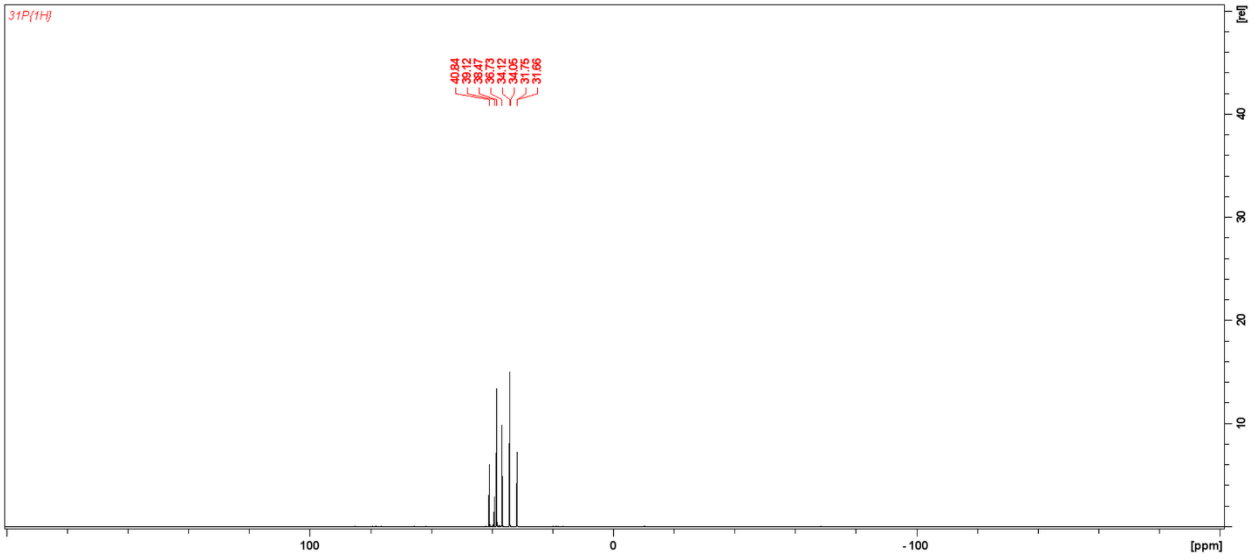

Figure S15. $^{31}P\{^{1}H\}$ NMR (THF-d_8, 162 MHz) spectrum of isolated white precipitate of $\{(Ph)_2(H)C\text{-}P\text{-}PtBu_2\}\{\mu^2\text{-}(S\text{-}C_6H_4\text{-}S)\}(tBu_2P\text{-}P\text{-}C(H)(Ph)_2\}$ (**3b**).

Mixture of two diastereomers:

- 39.66 ppm, d, $J_{P\text{-}P}$ = 384.4 Hz, $\{(Ph)_2(H)C\text{-}P\text{-}\mathbf{P}tBu_2\}\{\mu^2\text{-}(S\text{-}C_6H_4\text{-}S)\}\{tBu_2\mathbf{P}\text{-}P\text{-}C(H)(Ph)_2\}$;
- 32.94 ppm, d, $J_{P\text{-}P}$ = 384.4 Hz, $\{(Ph)_2(H)C\text{-}\mathbf{P}\text{-}PtBu_2\}\{\mu^2\text{-}(S\text{-}C_6H_4\text{-}S)\}\{tBu_2P\text{-}\mathbf{P}\text{-}C(H)(Ph)_2\}$;
- 37.93 ppm, d, $J_{P\text{-}P}$ = 387.3 Hz, $\{(Ph)_2(H)C\text{-}P\text{-}\mathbf{P}tBu_2\}\{\mu^2\text{-}(S\text{-}C_6H_4\text{-}S)\}\{tBu_2\mathbf{P}\text{-}P\text{-}C(H)(Ph)_2\}$;
- 32.86 ppm, d, $J_{P\text{-}P}$ = 387.3 Hz, $\{(Ph)_2(H)C\text{-}\mathbf{P}\text{-}PtBu_2\}\{\mu^2\text{-}(S\text{-}C_6H_4\text{-}S)\}\{tBu_2P\text{-}\mathbf{P}\text{-}C(H)(Ph)_2\}$;

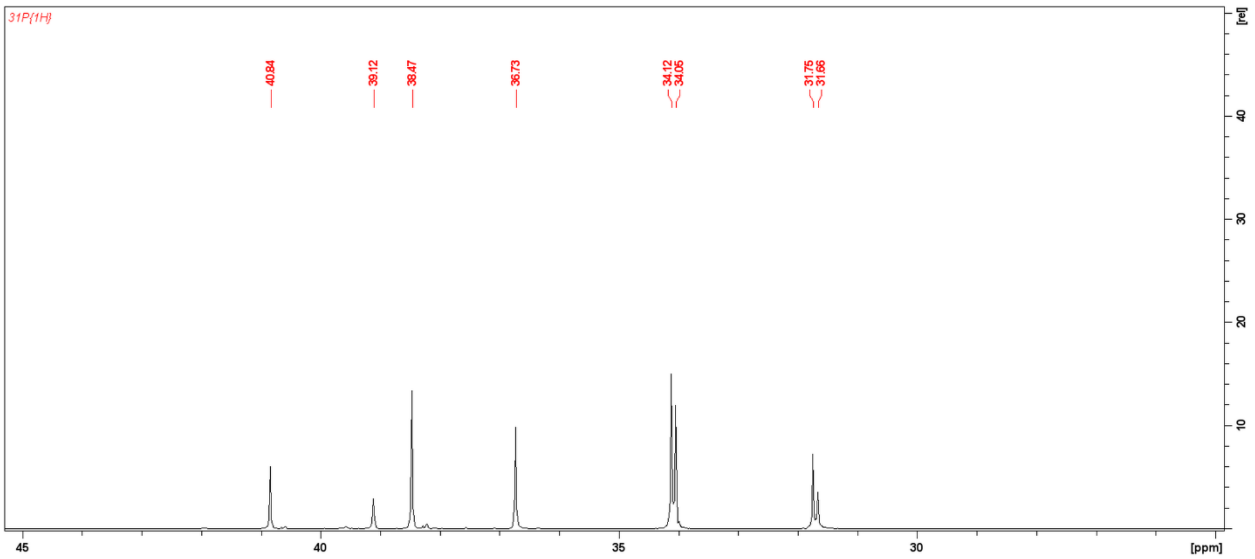

Figure S16. $^{31}P\{^{1}H\}$ NMR (THF-d_8, 162 MHz) spectrum of isolated white precipitate of $\{(Ph)_2(H)C\text{-}P\text{-}PtBu_2\}\{\mu^2\text{-}(S\text{-}C_6H_4\text{-}S)\}(tBu_2P\text{-}P\text{-}C(H)(Ph)_2\}$ (**3b**) in the range from 45 ppm to 25 ppm.

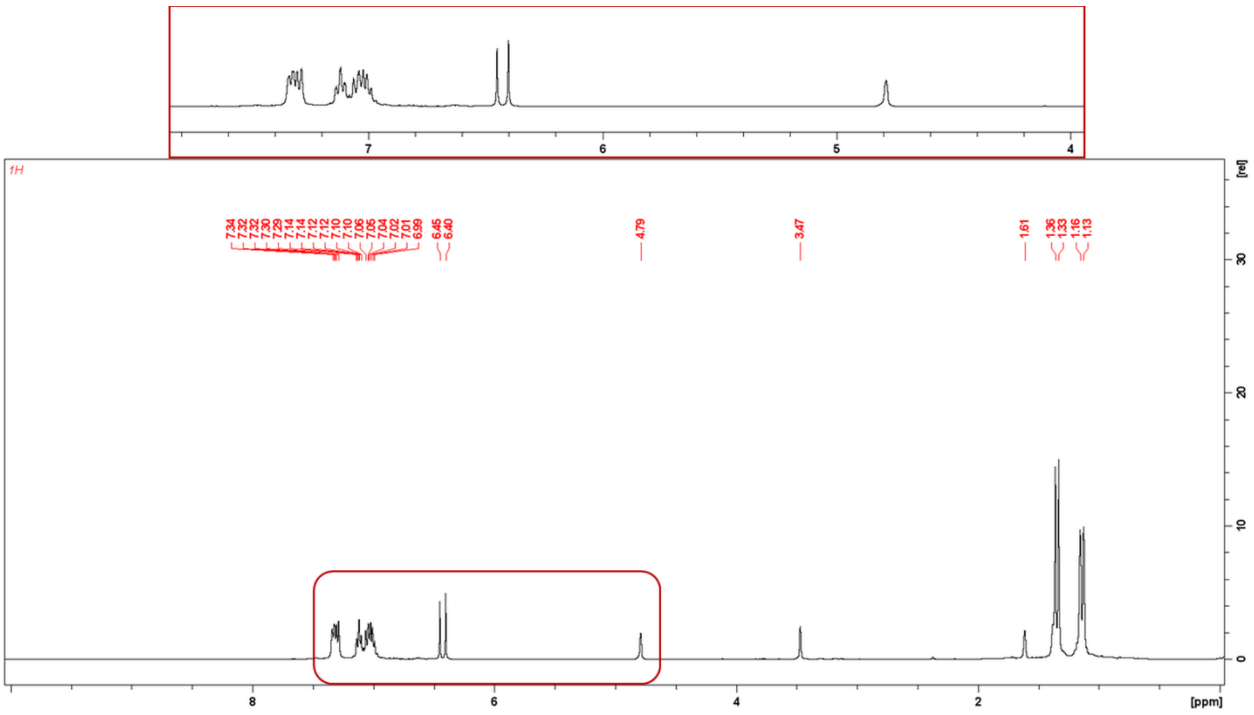

Figure S17. ^{1}H NMR (THF-d_8, 400 MHz) spectrum of isolated white precipitate of {(Ph)$_2$(H)C-P-P*t*Bu$_2$}{μ^2-(S-C$_6$H$_4$-S)}{*t*Bu$_2$P-P-C(H)(Ph)$_2$} (**3b**).

- 7.34 – 6.40 ppm, 24H, aromatic protons, {(**Ph**)$_2$(H)C-P-P*t*Bu$_2$}{μ^2-(S-C$_6$**H**$_4$-S)}{*t*Bu$_2$P-P-C(H)(**Ph**)$_2$};
- 4.79 ppm, broad s, 2 H, {(Ph)$_2$(**H**)C-P-P*t*Bu$_2$}{μ^2-(S-C$_6$H$_4$-S)}{*t*Bu$_2$P-P-C(**H**)(Ph)$_2$};
- 3.47 and 1.61 ppm, 4 H of THF;
- 1.34 ppm, d, $J_{P\text{-}H}$ = 11.6 Hz, 18H, {(Ph)$_2$(H)C-P-P***t*****Bu**$_2$}{μ^2-(S-C$_6$H$_4$-S)}{***t*****Bu**$_2$P-P-C(H)(Ph)$_2$}.
- 1.25 ppm, broad d, $J_{P\text{-}H}$ = 11.6 Hz, 18H, {(Ph)$_2$(H)C-P-P***t*****Bu**$_2$}{μ^2-(S-C$_6$H$_4$-S)}{***t*****Bu**$_2$P-P-C(H)(Ph)$_2$};

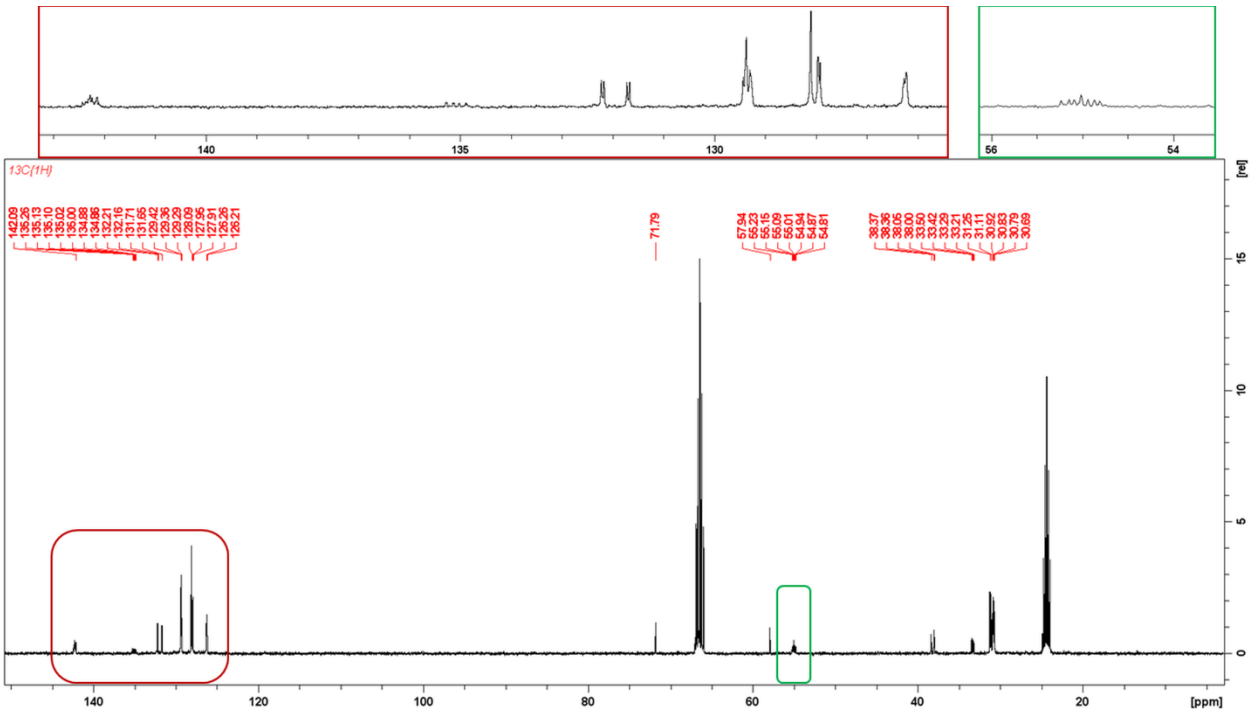

Figure S18. $^{13}C\{^{1}H\}$ NMR (THF-d_8, 100.62 MHz) spectrum of isolated white precipitate of $\{(Ph)_2(H)C\text{-}P\text{-}P\textit{t}Bu_2\}\{\mu^2\text{-}(S\text{-}C_6H_4\text{-}S)\}\{\textit{t}Bu_2P\text{-}P\text{-}C(H)(Ph)_2\}$ (**3b**).

Aromatic carbon atoms:

- 142.26 – 142.09 ppm, m;
- 135.06 ppm, ddd, $J_{P\text{-}C}$ = 24.4 Hz, $J_{P\text{-}C}$ = 13.5 Hz, $J_{P\text{-}C}$ = 1.9 Hz;
- 132.19 ppm, d, $J_{P\text{-}C}$ = 4.5 Hz;
- 131.68 ppm, dd, $J_{P\text{-}C}$ = 5.4 Hz;
- 129.72 ppm, d, $J_{P\text{-}C}$ = 12.7 Hz;
- 129.36 ppm, s;
- 128.09 ppm, s;
- 127.93 ppm, dd, $J_{P\text{-}C}$ = 4.5 Hz, $J_{P\text{-}C}$ = 0.9 Hz;
- 126.24 ppm, d, $J_{P\text{-}C}$ = 0.9 Hz;

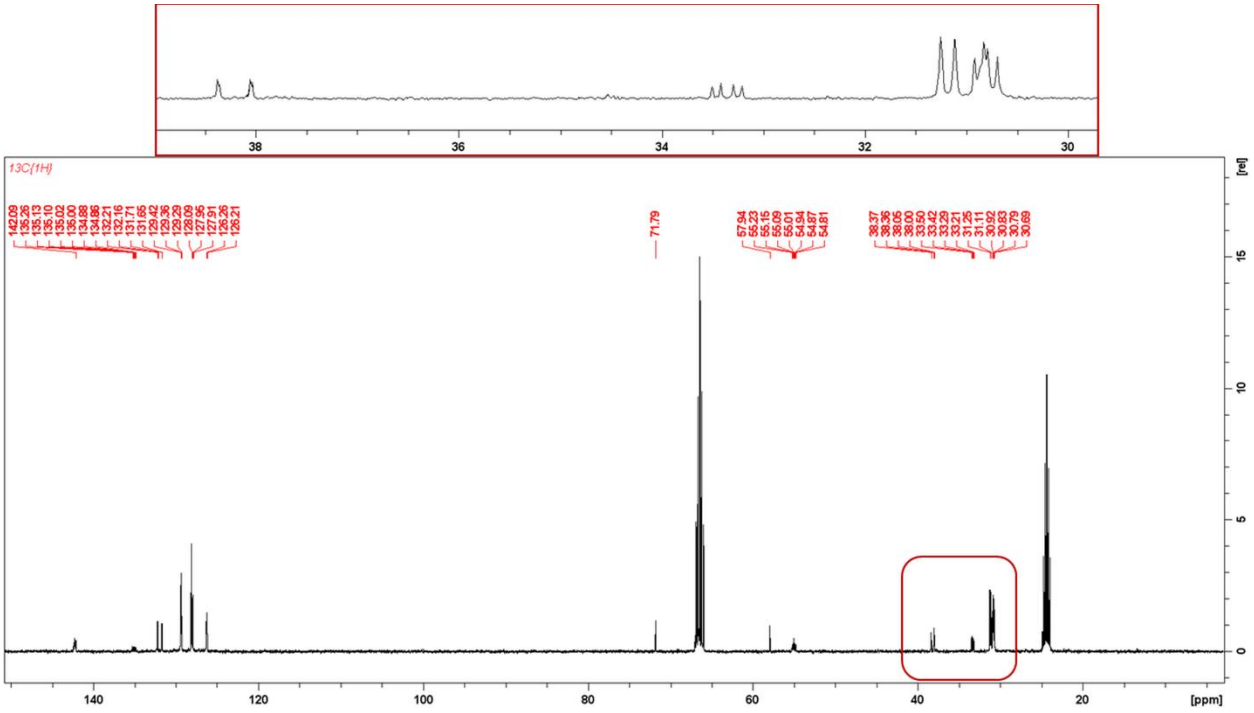

Figure S19. $^{13}C\{^{1}H\}$ NMR (THF-d_8, 100.62 MHz) spectrum of isolated white precipitate of $\{(Ph)_2(H)C\text{-}P\text{-}PtBu_2\}\{\mu^2\text{-}(S\text{-}C_6H_4\text{-}S)\}\{tBu_2P\text{-}P\text{-}C(H)(Ph)_2\}$ (**3b**).

- 55.01 ppm, ddd, $J_{P\text{-}C}$ = 21.6 Hz, $J_{P\text{-}C}$ = 14.5 Hz, $J_{P\text{-}C}$ = 8.2 Hz, $\{(Ph)_2(H)\mathbf{C}\text{-}P\text{-}PtBu_2\}\{\mu^2\text{-}(S\text{-}C_6H_4\text{-}S)\}\{tBu_2P\text{-}P\text{-}\mathbf{C}(H)(Ph)_2\}$;
- 38.2 ppm, dd, $J_{P\text{-}C}$ = 32.7 Hz, $J_{P\text{-}C}$ = 1.8 Hz, d, $\{(Ph)_2(H)C\text{-}P\text{-}P\{\mathbf{C}(CH_3)_3\}_2\}\{\mu^2\text{-}(S\text{-}C_6H_4\text{-}S)\}\{\{\mathbf{C}(CH_3)_3\}_2P\text{-}P\text{-}C(H)(Ph)_2\}$;
- 33.36 ppm, dd, $J_{P\text{-}C}$ = 20.9 Hz, $J_{P\text{-}C}$ = 8.2 Hz, $\{(Ph)_2(H)C\text{-}P\text{-}P\{\mathbf{C}(CH_3)_3\}_2\}\{\mu^2\text{-}(S\text{-}C_6H_4\text{-}S)\}\{\{\mathbf{C}(CH_3)_3\}_2P\text{-}P\text{-}C(H)(Ph)_2\}$;
- 31.17 ppm, dd, $J_{P\text{-}C}$ = 13.6 Hz, $J_{P\text{-}C}$ = 0.9 Hz, $\{(Ph)_2(H)C\text{-}P\text{-}P\{C(\mathbf{C}H_3)_3\}_2\}\{\mu^2\text{-}(S\text{-}C_6H_4\text{-}S)\}\{\{C(\mathbf{C}H_3)_3\}_2P\text{-}P\text{-}C(H)(Ph)_2\}$;
- 30.8 ppm, dd, $J_{P\text{-}C}$ = 13.6 Hz, $J_{P\text{-}C}$ = 9.0 Hz, $\{(Ph)_2(H)C\text{-}P\text{-}P\{C(\mathbf{C}H_3)_3\}_2\}\{\mu^2\text{-}(S\text{-}C_6H_4\text{-}S)\}\{\{C(\mathbf{C}H_3)_3\}_2P\text{-}P\text{-}C(H)(Ph)_2\}$;

B.1.4. Reaction of 1 with $HSCH_2C_6H_4CH_2SH$

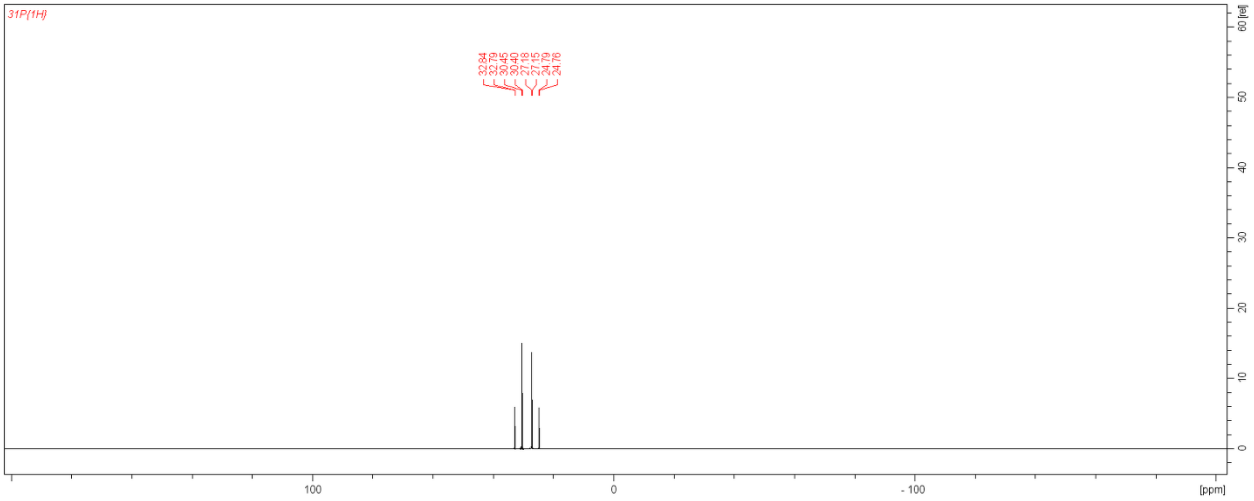

Figure S20. $^{31}P\{^{1}H\}$ NMR (C_6D_6, 162 MHz) spectrum of isolated crystals of $\{(Ph)_2(H)C\text{-}P\text{-}PtBu_2\}\{\mu^2\text{-}(S\text{-}CH_2\text{-}C_6H_4\text{-}CH_2\text{-}S)\}\{tBu_2P\text{-}P\text{-}C(H)(Ph)_2\}$ (**3c**).

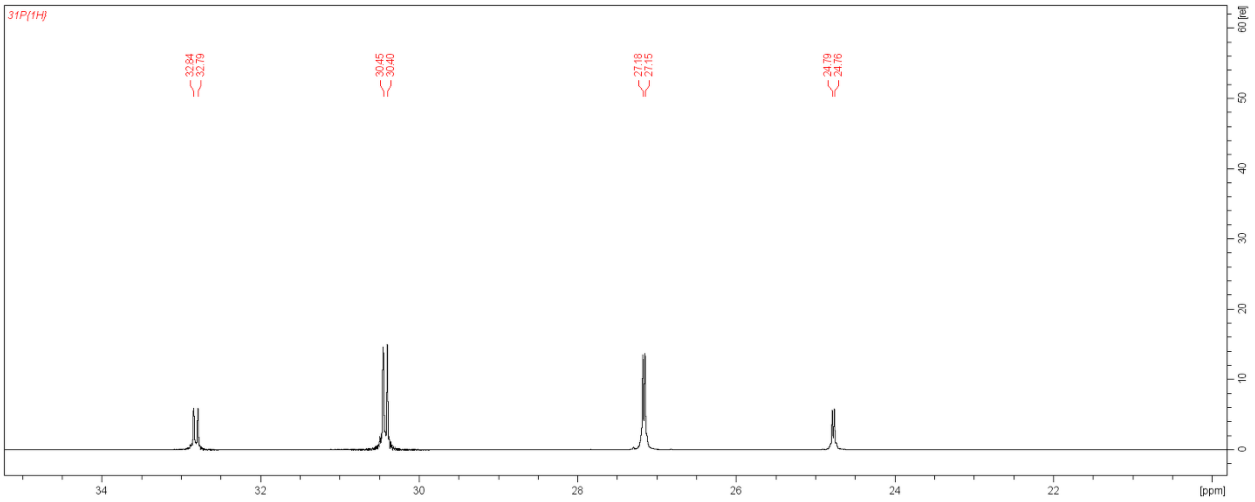

Figure S21. $^{31}P\{^{1}H\}$ NMR (C_6D_6, 162 MHz) spectrum of isolated crystals of {$(Ph)_2$(H)C-P-P*t*Bu_2}{μ^2-(S-CH_2-C_6H_4-CH_2-S)}{*t*Bu_2P-P-C(H)$(Ph)_2$} (**3c**) in the range from 35 ppm to 20 ppm.

Mixture of two diastereomers:

- 31.64 ppm, d, $J_{P\text{-}P}$ = 387.2 Hz, {$(Ph)_2$(H)C-P-**P***t*Bu_2}{μ^2-(S-CH_2-C_6H_4-CH_2-S)}{*t*Bu_2**P**-P-C(H)$(Ph)_2$};
- 25.96 ppm, d, $J_{P\text{-}P}$ = 387.2 Hz, {$(Ph)_2$(H)C-**P**-P*t*Bu_2}{μ^2-(S-CH_2-C_6H_4-CH_2-S)}{*t*Bu_2P-**P**-C(H)$(Ph)_2$};
- 31.59 ppm, d, $J_{P\text{-}P}$ = 386.0 Hz, {$(Ph)_2$(H)C-P-**P***t*Bu_2}{μ^2-(S-CH_2-C_6H_4-CH_2-S)}{*t*Bu_2**P**-P-C(H)$(Ph)_2$};
- 25.98 ppm, d, $J_{P\text{-}P}$ = 386.0 Hz, {$(Ph)_2$(H)C-**P**-P*t*Bu_2}{μ^2-(S-CH_2-C_6H_4-CH_2-S)}{*t*Bu_2P-**P**-C(H)$(Ph)_2$};

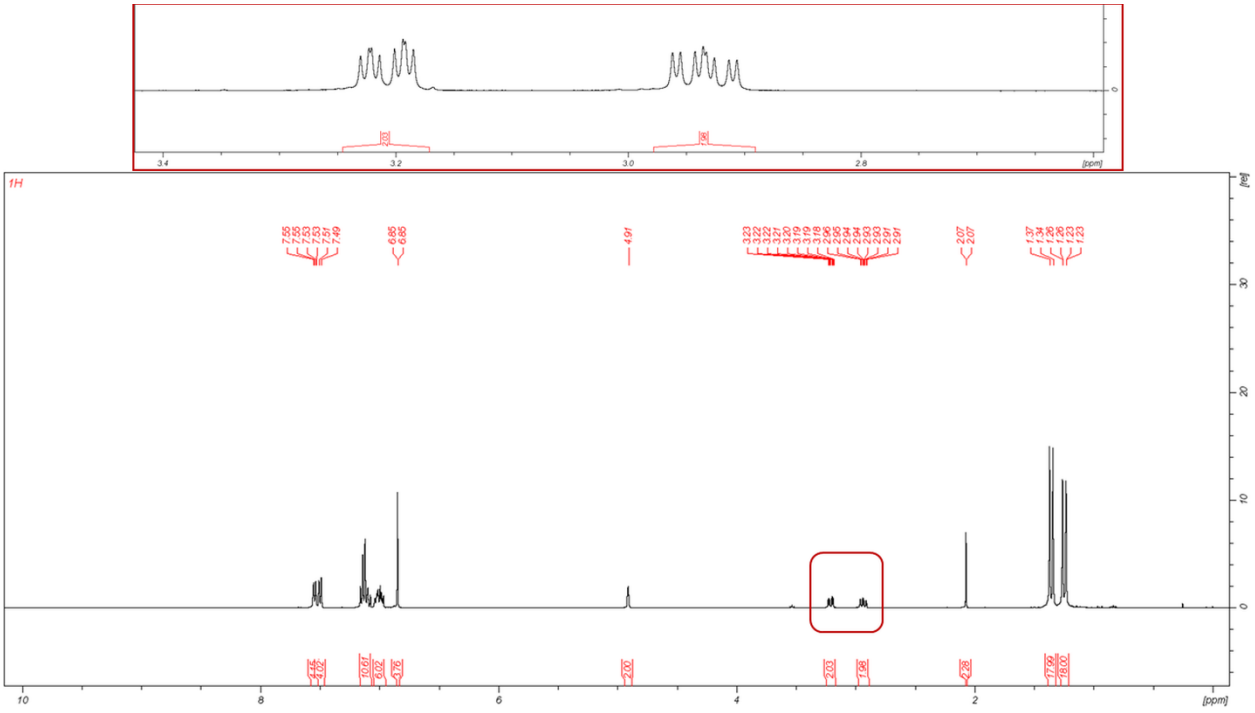

Figure S22. ^{1}H NMR (C_6D_6, 400 MHz) spectrum of isolated crystals of {$(Ph)_2$(H)C-P-P*t*Bu_2}{μ^2-(S-CH_2-C_6H_4-CH_2-S)}{*t*Bu_2P-P-C(H)$(Ph)_2$} (**3c**).

- 7.55 – 6.96 ppm, 24H, aromatic protons, {(**Ph**)$_2$(H)C-P-P*t*Bu_2}{μ^2-(S-CH_2-C_6**H**$_4$-CH_2-S)}{*t*Bu_2P-P-C(H)(**Ph**)$_2$};
- 6.85 and 2.07 ppm, 8H, residual amounts of toluene used in the synthesis;
- 4.91 ppm, broad t, $J_{P\text{-}H}$ = 2.3Hz, 2 H, {$(Ph)_2$(**H**)C-P-P*t*Bu_2}{μ^2-(S-CH_2-C_6H_4-CH_2-S)}{*t*Bu_2P-P-C(**H**)$(Ph)_2$};
- 3.21 ppm, qd, $J_{H\text{-}H}$ = 11.7 Hz, $J_{H\text{-}H}$ = 3.7 Hz, $J_{P\text{-}H}$ = 2.8 Hz, 2H, {$(Ph)_2$(H)C-P-P*t*Bu_2}{μ^2-(S-C**H**$_2$-C_6H_4-C**H**$_2$-S)}{*t*Bu_2P-P-C(H)$(Ph)_2$};
- 2.93 ppm, qd, $J_{H\text{-}H}$ = 11.7 Hz, $J_{H\text{-}H}$ = 7.8 Hz, $J_{P\text{-}H}$ = 2.8 Hz, 2H, {$(Ph)_2$(H)C-P-P*t*Bu_2}{μ^2-(S-C**H**$_2$-C_6H_4-C**H**$_2$-S)}{*t*Bu_2P-P-C(H)$(Ph)_2$};
- 1.35 ppm, d, $J_{P\text{-}H}$ = 11.7 Hz, 18H, {$(Ph)_2$(H)C-P-P***t*****Bu**$_2$}{μ^2-(S-CH_2-C_6H_4-CH_2-S)}{***t*****Bu**$_2$P-P-C(H)$(Ph)_2$};
- 1.25 ppm, dd, $J_{P\text{-}H}$ = 11.4 Hz, $J_{P\text{-}H}$ = 1.4 Hz, 18H, {$(Ph)_2$(H)C-P-P***t*****Bu**$_2$}{μ^2-(S-CH_2-C_6H_4-CH_2-S)}{***t*****Bu**$_2$P-P-C(H)$(Ph)_2$};

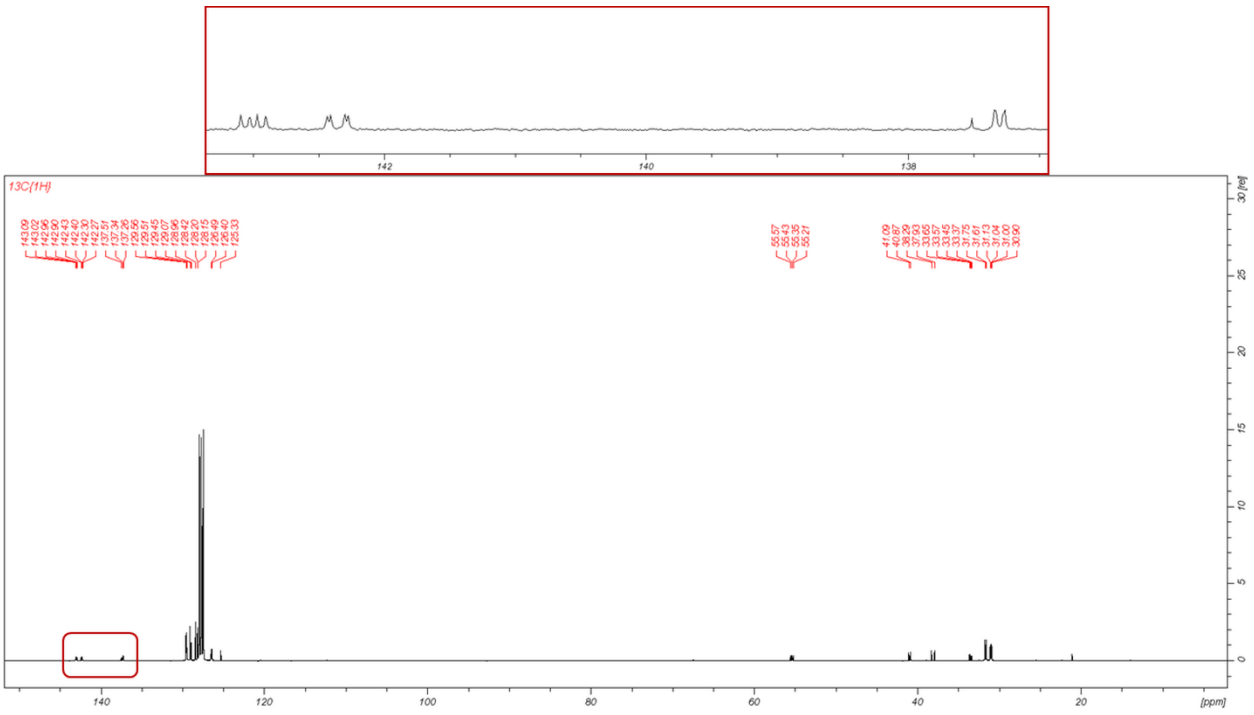

Figure S23. $^{13}C\{^{1}H\}$ NMR (C_6D_6, 100.62 MHz) spectrum of isolated crystals of {$(Ph)_2$(H)C-P-P*t*Bu_2}{μ^2-(S-CH_2-C_6H_4-CH_2-S)}{*t*Bu_2P-P-C(H)$(Ph)_2$} (**3c**).

Aromatic carbon atoms:

- 142.99 ppm, dd, $J_{P\text{-}C}$ = 13.0 Hz, $J_{P\text{-}C}$ = 6.7 Hz;
- 142.35 ppm, dd, $J_{P\text{-}C}$ = 13.6 Hz, $J_{P\text{-}C}$ = 2.7 Hz;
- 137.51 ppm, s;
- 137.31 ppm, dd, $J_{P\text{-}C}$ = 6.9 Hz, $J_{P\text{-}C}$ = 1.3 Hz;
- 129.54 ppm, d, $J_{P\text{-}C}$ = 5.8 Hz;
- 129.49 ppm, d, $J_{P\text{-}C}$ = 10.2 Hz;
- 129.45 ppm, d, $J_{P\text{-}C}$ = 2.0 Hz;
- 129.07 ppm, s:
- 128.96 ppm, s;
- 128.42 ppm, s;
- 128.20 ppm, s;
- 128.15 ppm, s;
- 126.49 ppm, d, $J_{P\text{-}C}$ = 1.8 Hz;
- 126.39 ppm, d, $J_{P\text{-}C}$ = 2.2 Hz;
- 125.33 ppm, s;

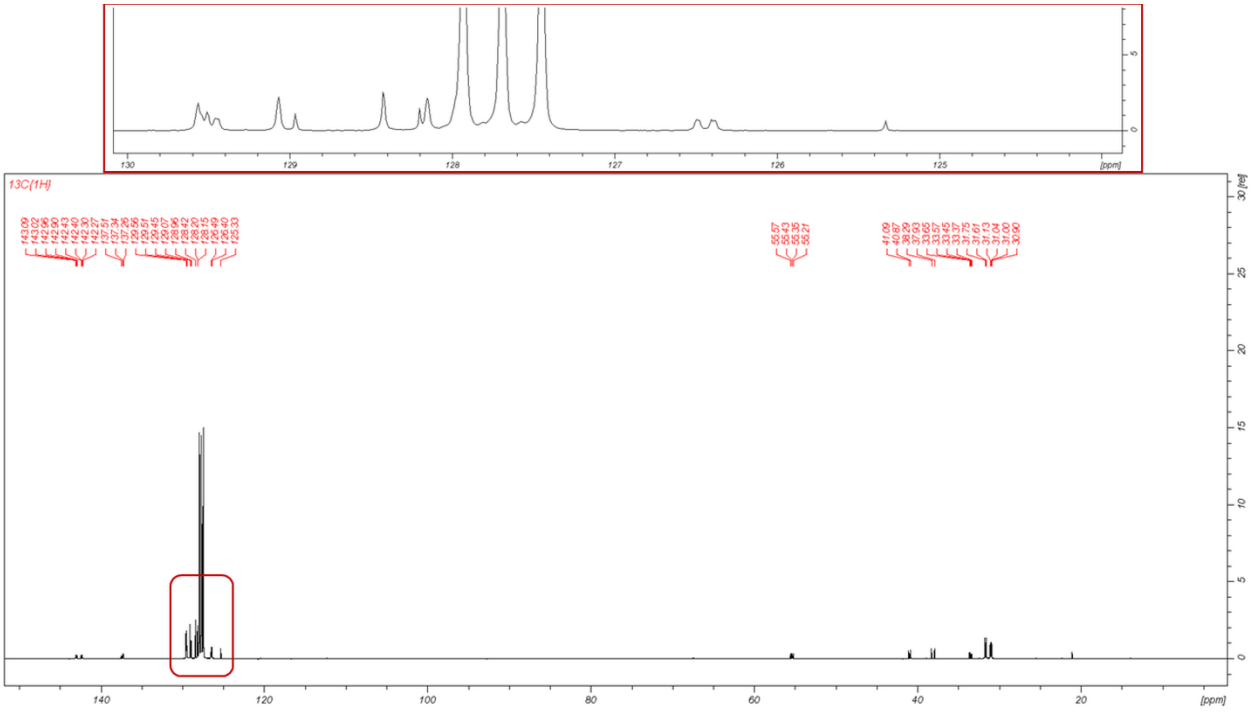

Figure S24. $^{13}C\{^{1}H\}$ NMR (C_6D_6, 100.62 MHz) spectrum of isolated crystals of $\{(Ph)_2(H)C\text{-}P\text{-}PtBu_2\}\{\mu^2\text{-}(S\text{-}CH_2\text{-}C_6H_4\text{-}CH_2\text{-}S)\}\{tBu_2P\text{-}P\text{-}C(H)(Ph)_2\}$ (**3c**).

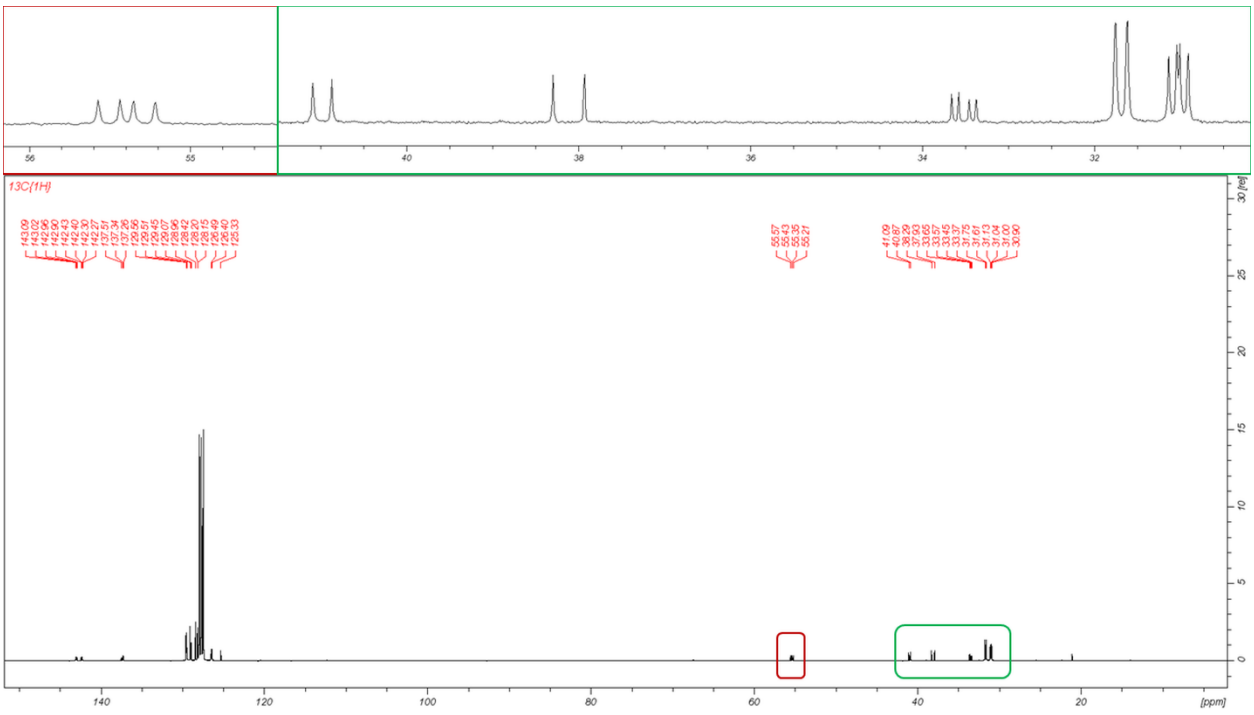

Figure S25. $^{13}C\{^{1}H\}$ NMR (C_6D_6, 100.62 MHz) spectrum of isolated crystals of $\{(Ph)_2(H)C\text{-}P\text{-}PtBu_2\}\{\mu^2\text{-}(S\text{-}CH_2\text{-}C_6H_4\text{-}CH_2\text{-}S)\}\{tBu_2P\text{-}P\text{-}C(H)(Ph)_2\}$ (**3c**).

- 55.39 ppm, dd, $J_{P\text{-}C}$ = 22.0 Hz, $J_{P\text{-}C}$ = 13.6 Hz, $\{(Ph)_2(H)\mathbf{C}\text{-}P\text{-}PtBu_2\}\{\mu^2\text{-}(S\text{-}CH_2\text{-}C_6H_4\text{-}CH_2\text{-}S)\}\{tBu_2P\text{-}P\text{-}\mathbf{C}(H)(Ph)_2\}$;
- 40.98 ppm, d, $J_{P\text{-}C}$ = 13.6 Hz, $\{(Ph)_2(H)C\text{-}P\text{-}PtBu_2\}\{\mu^2\text{-}(S\text{-}\mathbf{C}H_2\text{-}C_6H_4\text{-}\mathbf{C}H_2\text{-}S)\}\{tBu_2P\text{-}P\text{-}C(H)(Ph)_2\}$;
- 38.11 ppm, d, $J_{P\text{-}C}$ = 36.8 Hz, d, $\{(Ph)_2(H)C\text{-}P\text{-}P\{\mathbf{C}(CH_3)_3\}_2\}\{\mu^2\text{-}(S\text{-}CH_2\text{-}C_6H_4\text{-}CH_2\text{-}S)\}\{\{\mathbf{C}(CH_3)_3\}_2P\text{-}P\text{-}C(H)(Ph)_2\}$;
- 33.52 ppm, dd, $J_{P\text{-}C}$ = 20.4 Hz, $J_{P\text{-}C}$ = 8.1 Hz, $\{(Ph)_2(H)C\text{-}P\text{-}P\{\mathbf{C}(CH_3)_3\}_2\}\{\mu^2\text{-}(S\text{-}CH_2\text{-}C_6H_4\text{-}CH_2\text{-}S)\}\{\{\mathbf{C}(CH_3)_3\}_2P\text{-}P\text{-}C(H)(Ph)_2\}$;
- 31.69 ppm, dd, $J_{P\text{-}C}$ = 13.7 Hz, $J_{P\text{-}C}$ = 1.22 Hz, $\{(Ph)_2(H)C\text{-}P\text{-}P\{C(\mathbf{C}H_3)_3\}_2\}\{\mu^2\text{-}(S\text{-}CH_2\text{-}C_6H_4\text{-}CH_2\text{-}S)\}\{\{C(\mathbf{C}H_3)_3\}_2P\text{-}P\text{-}C(H)(Ph)_2\}$;
- 31.02 ppm, dd, $J_{P\text{-}C}$ = 13.0 Hz, $J_{P\text{-}C}$ = 9.7 Hz, $\{(Ph)_2(H)C\text{-}P\text{-}P\{C(\mathbf{C}H_3)_3\}_2\}\{\mu^2\text{-}(S\text{-}CH_2\text{-}C_6H_4\text{-}CH_2\text{-}S)\}\{\{C(\mathbf{C}H_3)_3\}_2P\text{-}P\text{-}C(H)(Ph)_2\}$;
- 21.08 ppm, methyl groups carbon atom from toluene;

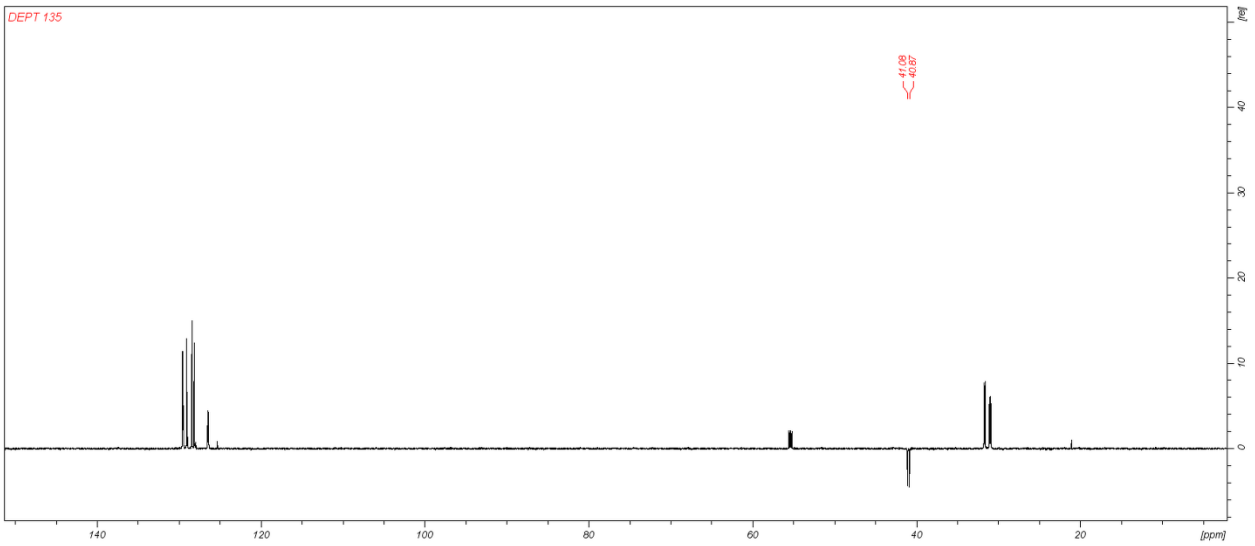

Figure S26. $^{13}C\{^{1}H\}$ NMR-dept135 (C_6D_6, 100.62 MHz) spectrum of isolated crystals of {$(Ph)_2$(H)C-P-P*t*Bu_2}{μ^2-(S-CH_2-C_6H_4-CH_2-S)}{*t*Bu_2P-P-C(H)$(Ph)_2$} (**3c**).

B.2. Solid state NMR

NMR experiments were performed using a Jeol JNM-ECZ500R 500 MHz spectrometer equipped with an AUTOMAS 3.2 mm solid state probe. Samples consisting of 75–100 mg were spun in a Joel 3.2 mm of. zirconium oxide rotor at a spinning rate of 10000 Hz. A single contact cross polarization technique was employed using a contact time of 2 ms (recycled delay time 5s) with proton decoupling during the acquisition period. All measurements were conducted at 300K. NaH_2PO_4 was used as the standard for ^{31}P MAS NMR measurements.

B.2.1. Crystals of *rac*-poly_3a_Cu

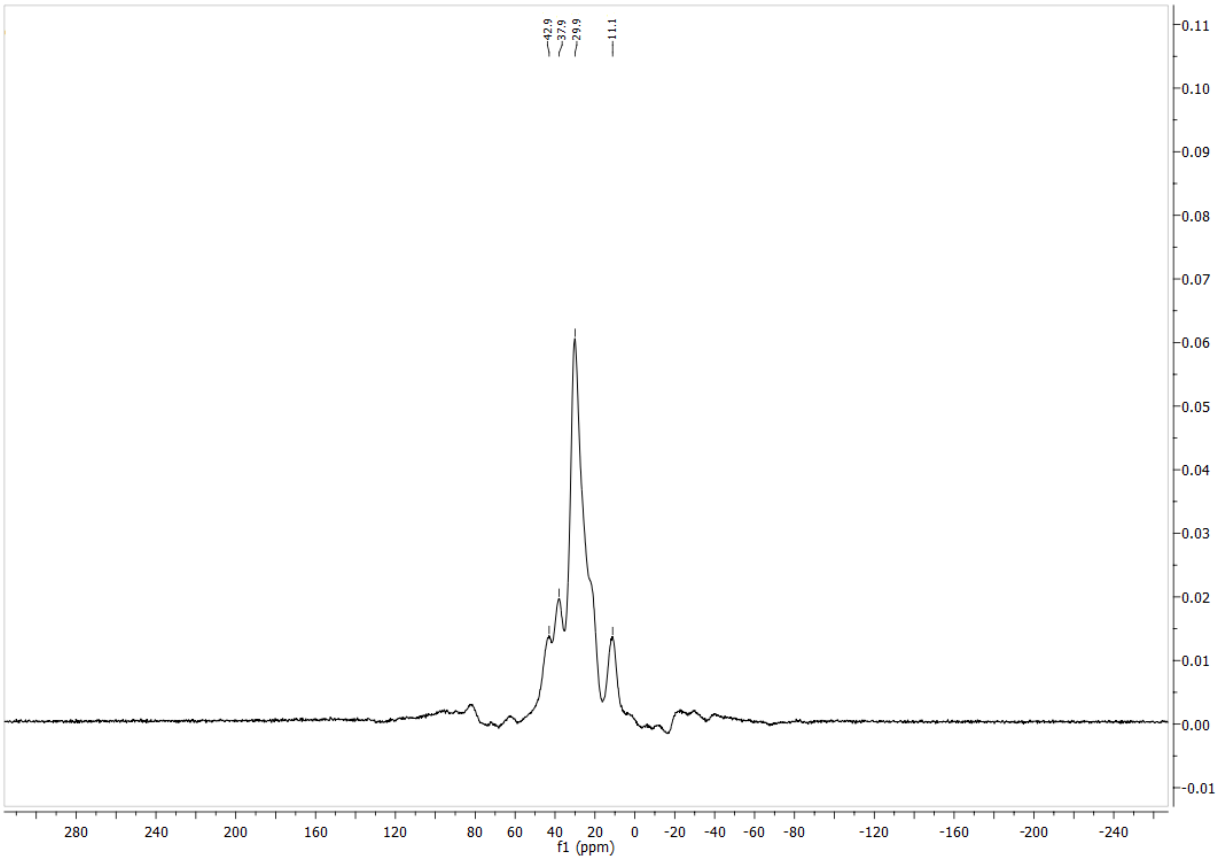

Figure S27. ^{31}P CPMAS spectrum of ***rac*-poly_3a_Cu**.

B.2.2. Crystals of *meso*-poly_3a_Ag

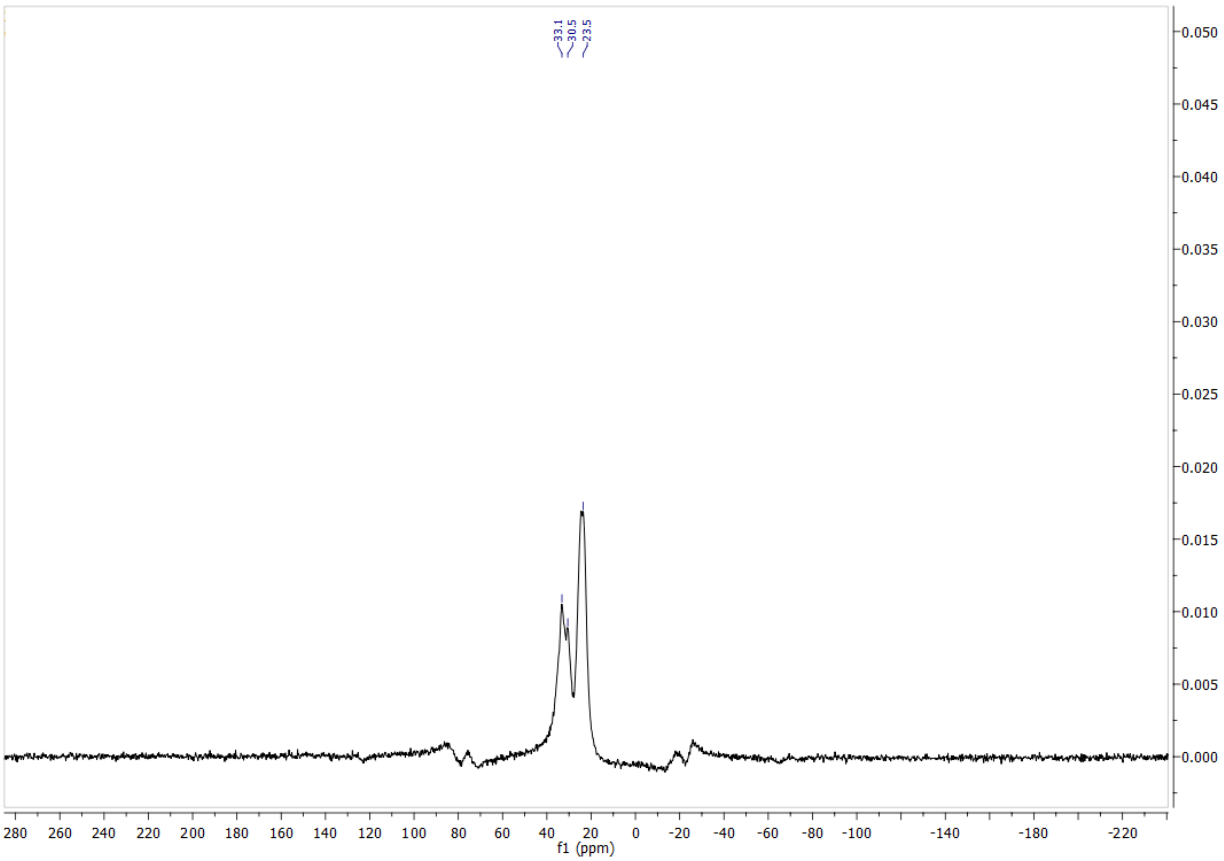

Figure S28. ^{31}P CPMAS spectrum of ***meso*-poly_3a_Ag**.

B.2.3. Crystals of *rac*-poly_3c_Cu

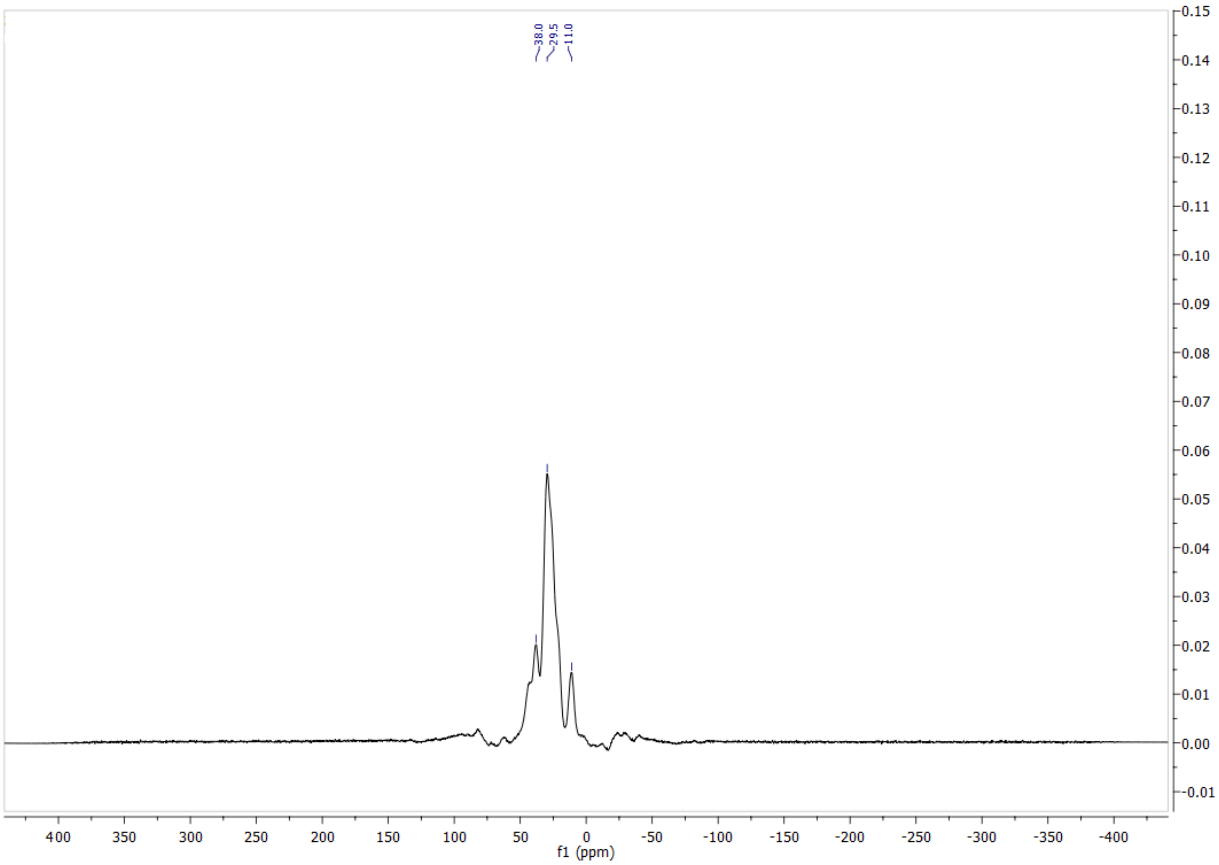

Figure S29. ^{31}P CPMAS spectrum of ***rac*-poly_3c_Cu**.

B.2.4. Crystals of *rac*-poly_3c_Ag

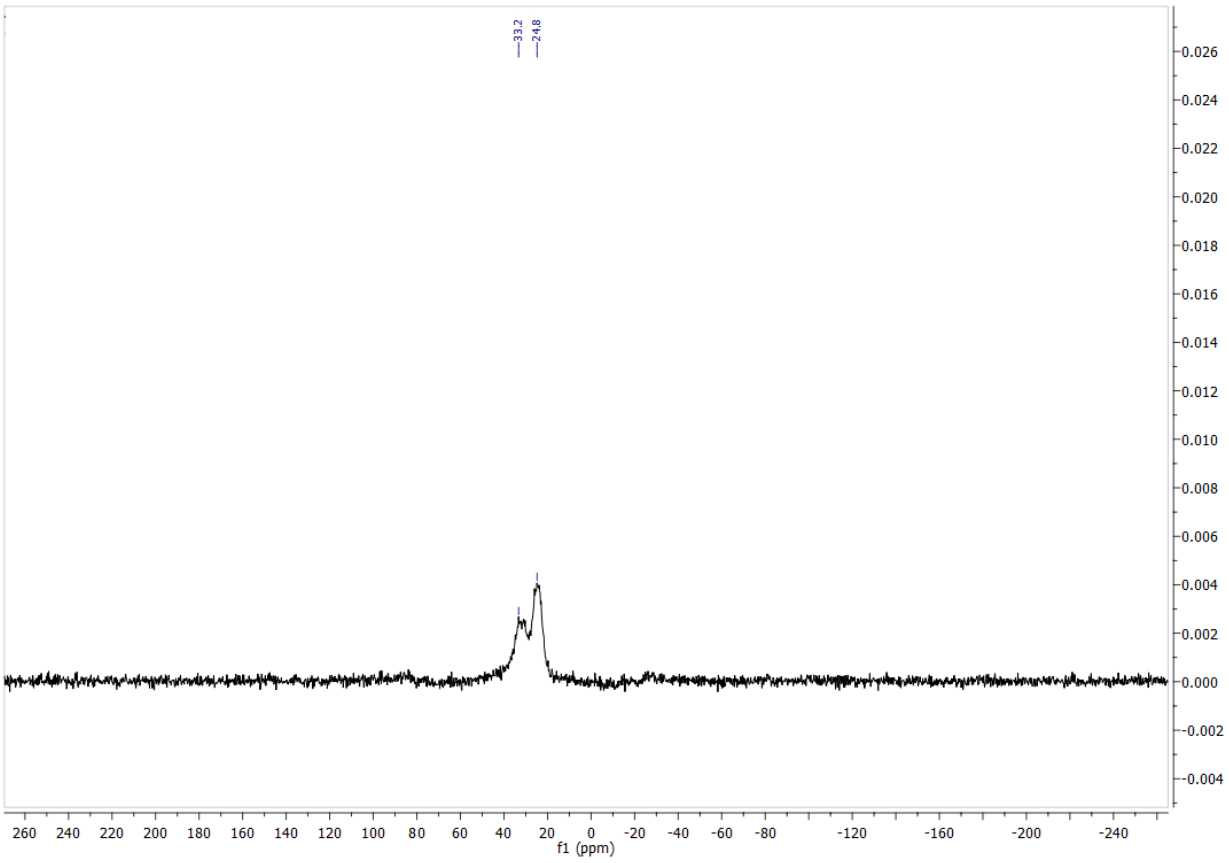

Figure S30. ^{31}P CPMAS spectrum of ***rac*-poly_3c_Ag**.

PART B. X-ray data

The X-ray intensity data for were measured with an IPDS2T diffractometer equipped with an STOE image plate detector system and microfocus X-ray sources providing Kα radiation by high-grade multilayer X-ray mirror optics for Mo (λ = 0.71073 Å, **3c**, ***rac*-poly_3a_Cu** and) and Cu (λ = 1.54186 Å, **3a**, ***meso*-poly_3a_Ag**) wavelengths. The X-ray intensity data for ***rac*-poly_3c_Cu** and ***rac*-poly_3c_Ag_*RR*** and ***rac*-poly_3c_Ag_*SS*** were measured with an STADIVARI diffractometer from STOE equipped with an EGER 1M CDTE detector and AXO_Mo sources providing Kα radiation by high-grade multilayer X-ray mirror optics for Mo (λ = 0.71073 Å) wavelengths. The measurements were carried out at 120 K. The structures of the compounds were solved by direct methods and refined against F^2 with the Shelxs-2008 and Shelxl-2008 programs[2] run under WinGX.[3] Non-hydrogen atoms were refined with anisotropic displacement parameters. The isotropic displacement parameters of all hydrogens were fixed to 1.2 U_{eq} for aromatic, CH, CH_2 (1.5 times for methyl) groups.

The crystallographic data for all structures reported in this paper have been deposited in the Cambridge Crystallographic Data Centre as supplementary publication No. CCDC 2307097-2307103. Copies of the data can be obtained free of charge upon application to the CCDC, 12 Union Road, Cambridge CB2 1EZ, UK (Fax: (+44) 1223-336-033; E mail: deposit@ccdc.cam.ac.uk).

Table S1. Crystallographic data for **3a** and **3c**.

	3a	**3c**
Empirical formula	$C_{46}H_{66}P_4S_2$	$C_{57}H_{75}P_4S_2$
Formula weight	806.98	947.16
Radiation source	Cu-*Kα*	Mo-*Kα*
Wavelength [Å]	1.54186	0.71073
Crystal System	Triclinic	Triclinic
Space group	*P*-1	*P*-1
a [Å]	8.4421(4)	9.6607(4)
b [Å]	9.3290(4)	17.1058(7)
c [Å]	16.0163(7)	17.4524(7)
α [°]	80.560(3)	105.193(3)
β [°]	88.671(4)	94.859(3)
γ [°]	66.536(3)	101.727(3)
V [Å3]	1140.18(9)	2696.0(2)
Z	1	2
Calculated Density [g·cm-1]	1.175	1.167
T [K]	120(2)	120(2)
μ [mm-1]	2.599	0.253
Theta range for data collection [°]	2.80-67.90	2.18-29.72
Index ranges	$-8 \le h \le 8$ $-10 \le k \le 10$ $-18 \le l \le 18$	$-11 \le h \le 13$ $-23 \le k \le 23$ $-22 \le l \le 23$
Data / restraints / parameters	3721/0/241	14459/0/585
Goodness-of-fit on F^2	1.047	1.065
Final R indices	0.031	0.0702
[*I*>2σ(I)]	0.0348	0.1126
R indices (all data)	0.0792	0.1126
[*I*>2σ(I)] (all data)	0.0825	0.1742
Largest diff. peak and hole [e.Å-3]	0.242 and -0.283	0.679 and -0.475
CCDC	**2307103**	**2307101**

Table S2. Crystallographic data for ***rac*-poly_3a_Cu**, ***meso*-poly_3a_Ag** and ***rac*-poly_3c_Cu**.

	***rac*-poly_3a_Cu**	***meso*-poly_3a_Ag**	***rac*-poly_3c_Cu**
Empirical formula	$C_{23}H_{32}ClCuP_2S$	$C_{23}H_{33}AgClP_2S$	$C_{25}H_{33}ClCuP_2S$
Formula weight	502.48	546.81	526.5
Radiation source	Mo-*Kα*	Cu-*Kα*	Mo-*Kα*
Wavelength [Å]	0.71073	1.54186	0.71073
Crystal System	Monoclinic	Triclinic	Monoclinic
Space group	*I*2/a	*P*-1	*I*2/a
a [Å]	17.2149(13)	8.6692(4)	28.5608(14)
b [Å]	9.9874(6)	9.7343(4)	9.7959(4)
c [Å]	29.208(2)	16.9516(8)	18.4297(8)
α [°]	90	90.826(4)	90
β [°]	105.951(6)	103.141(3)	99.998(4)
γ [°]	90	115.892(3)	90
V [Å3]	4828.4(6)	1242.62(10)	5077.9(4)
Z	8	2	8
Calculated Density [g·cm-1]	1.382	1.462	1.377
T [K]	120(2)	120(2)	120(2)
μ [mm-1]	1.242	9.538	1.184
Theta range for data collection [°]	2.61-27.80	2.70-67.92	2.87- 29.57
Index ranges	$-22 \le h \le 23$ $-13 \le k \le 13$ $-40 \le l \le 39$	$-10 \le h \le 10$ $-11 \le k \le 11$ $-19 \le l \le 19$	$-39 \le h \le 37$ $-12 \le k \le 13$ $-22 \le l \le 24$
Data / restraints / parameters	6468/0/288	4118/0/259	5996/0/277
Goodness-of-fit on F^2	1.039	1.089	1.025
Final R indices	0.0767	0.0632	0.0617
[I>2σ(I)]	0.1792	0.1693	0.1444
R indices (all data)	0.1818	0.0668	0.1234
[I>2σ(I)] (all data)	0.2257	0.173	0.1695
Largest diff. peak and hole [e.Å-3]	0.111 and -1.059	0.15 and -1.677	0.124 and -0.697
CCDC	**2307099**	**2307098**	**2307097**

Table S3. Crystallographic data for ***rac*-poly_3c_Ag_*RR*** and ***rac*-poly_3c_Ag_*SS***.

	rac*-poly_3c_Ag_*RR	***rac*-poly_3c_Ag_*SS***
Empirical formula	$C_{25}H_{33}AgClP_2S$	$C_{25}H_{33}AgClP_2S$
Formula weight	570.83	570.83
Radiation source	Mo-*Kα*	Mo-*Kα*
Wavelength [Å]	0.71073	0.71073
Crystal System	Monoclinic	Monoclinic
Space group	*I*2/a	*I*2/a
a [Å]	29.1911(18)	29.324(3)
b [Å]	9.7656(4)	9.7516(6)
c [Å]	18.4336(12)	18.3994(14)
α [°]	90	90
β [°]	98.632(5)	98.631(7)
γ [°]	90	90
V [Å3]	5195.3(5)	6750
Z	8	8
Calculated Density [g·cm-1]	1.46	1.458
T [K]	150(2)	120(2)
μ [mm-1]	1.093	1.092
Theta range for data collection [°]	3.06-29.70	2.84-26.12
Index ranges	-38 ≤ h ≤ 36 -10 ≤ k ≤ 12 -22 ≤ l ≤ 25	-37 ≤ h ≤ 38 -10 ≤ k ≤ 13 -25 ≤ l ≤ 23
Data / restraints / parameters	5668/0/277	6290/0/277
Goodness-of-fit on F^2	1.032	1.006
Final R indices	0.0644	0.0743
[*I*>2σ(I)]	0.1567	0.1436
R indices (all data)	0.1439	0.2291
[*I*>2σ(I)] (all data)	0.193	0.1964
Largest diff. peak and hole [e.Å-3]	0.148 and -1.099	0.137 and -0.906
CCDC	**2307100**	**2307102**

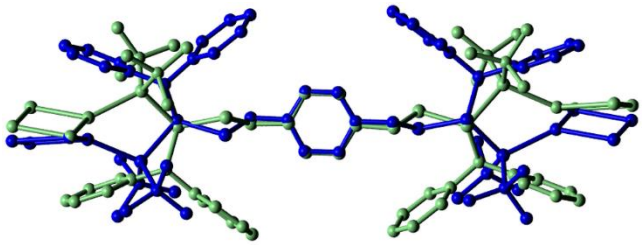

Figure S31. Overlay of the two basic units of the polymer ***rac*-poly_3c_Ag** (blue: *RR* configuration, mint: *SS* configuration).

PART C. TG and DSC spectra

Thermogravimetric analysis (TG) was carried out under argon atmosphere with a flow rate of 60 ml/min in the temperature range 35–800 °C (heating rate 5°C/min) using STA 449 F1 (Netzsch). The differential scanning calorimetry (DSC) measurement was performed under an argon atmosphere with a flow rate 60 mL min/1 in the temperature range of 35–600 °C (with a heating rate of 10 °C min–1) using a NETZSCH DSC 204 F1 Phoenix calorimeter. A constant sample mass of 2±0.5 mg was maintained throughout the TG and DSC analysis.

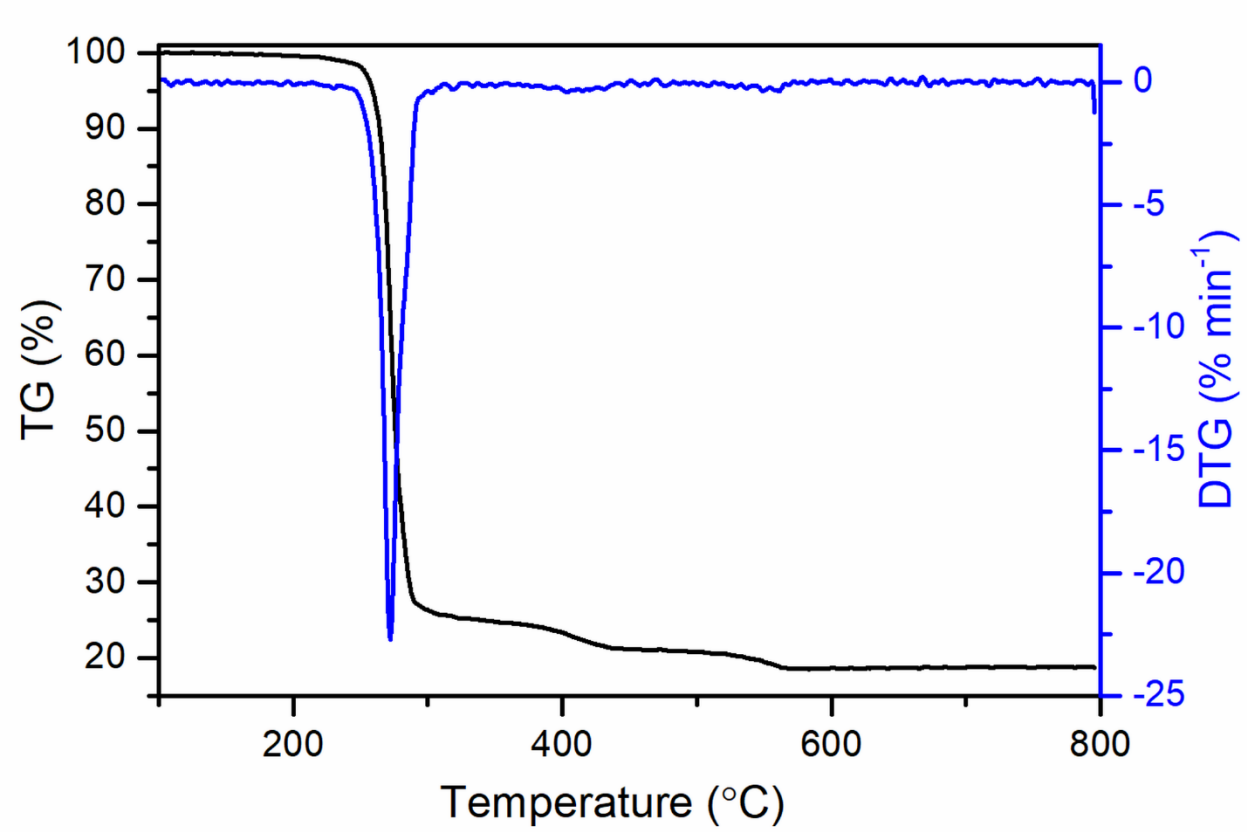

Figure S32. TG-DTG curve of the ***rac*-poly_3a_Cu** in a temperature range from 35°C to 300°C with a heating rate of 5°Cmin^{-1} (the black lines represent the TG curves, while the blue lines represent the first derivatives of the TG curves – DTG).

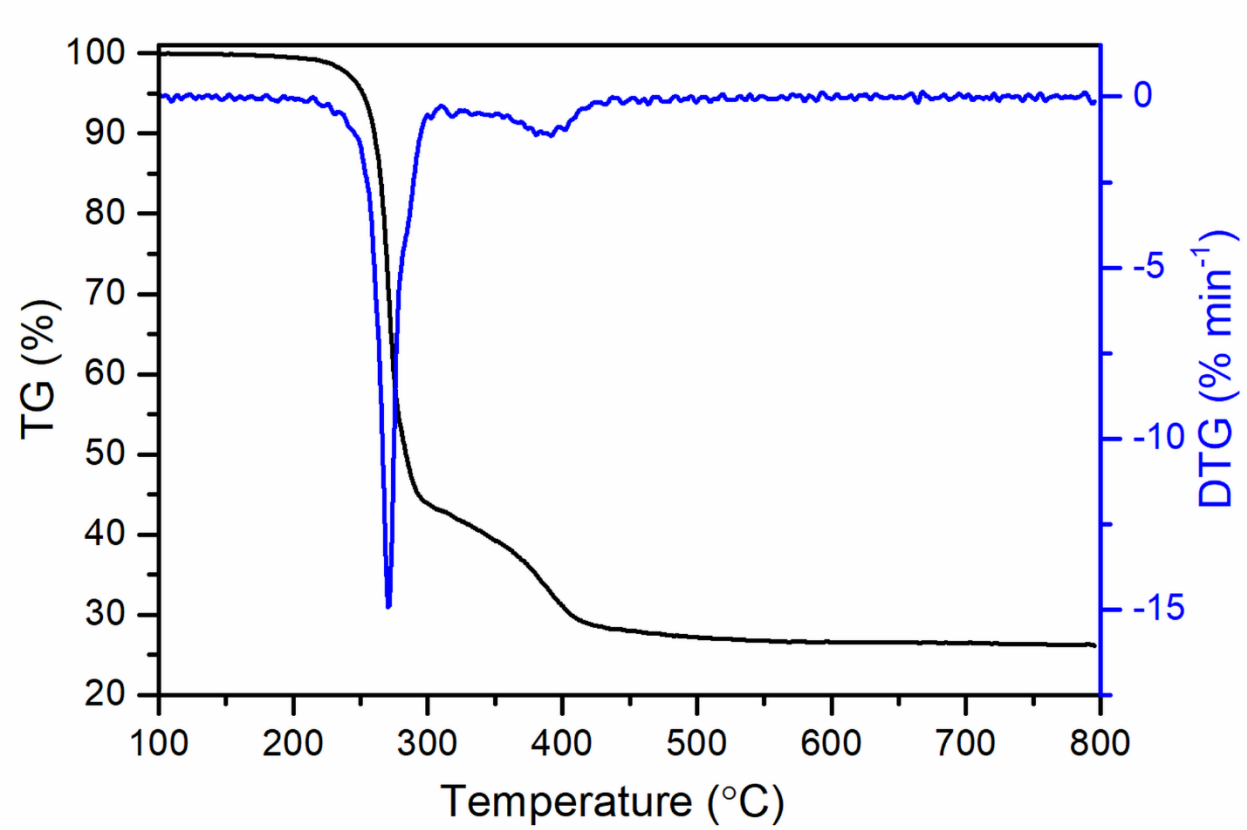

Figure S33. TG-DTG curve of the ***rac*-poly_3c_Cu** in a temperature range from 35°C to 300°C with a heating rate of 5°Cmin^{-1}(the black lines represent the TG curves, while the blue lines represent the first derivatives of the TG curves – DTG).

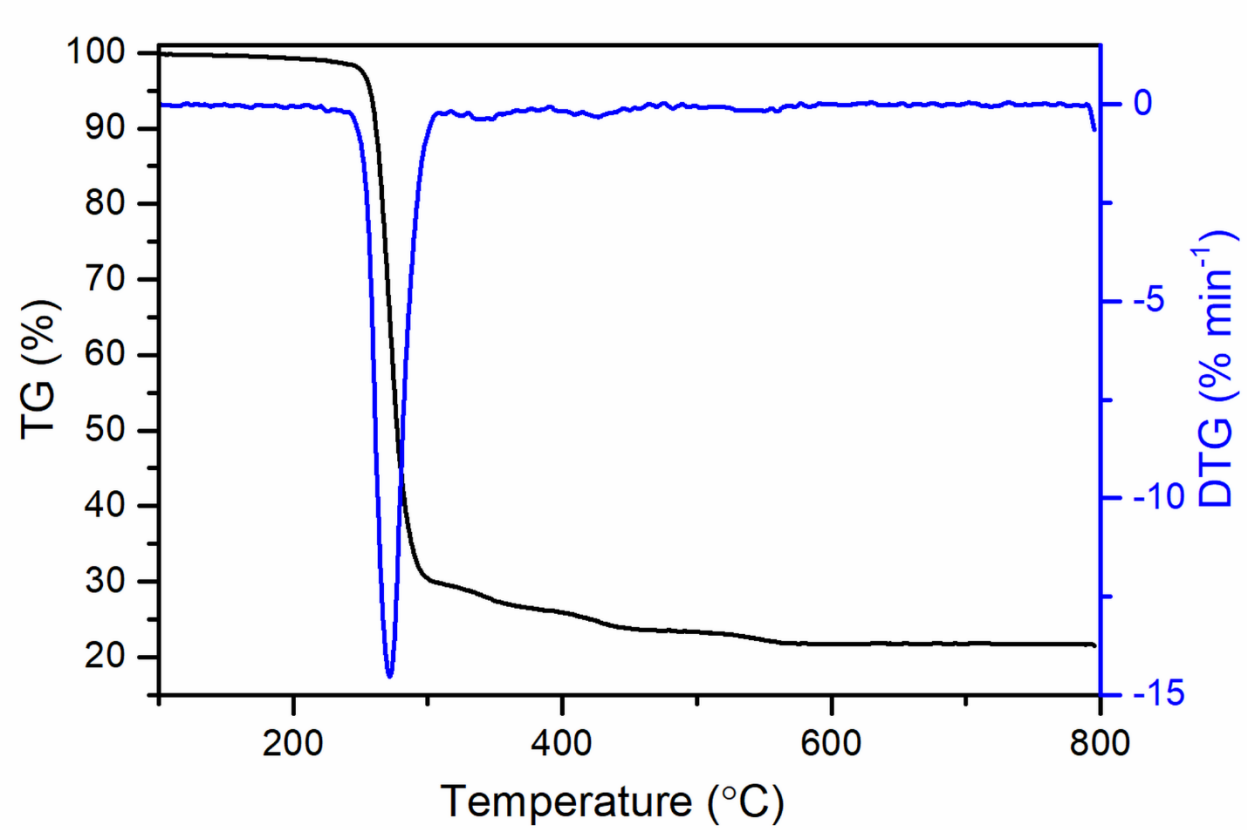

Figure S34. TG-DTG curve of the ***meso*-poly_3a_Ag** in a temperature range from 35°C to 300°C with a heating rate of 5°Cmin^{-1}(the black lines represent the TG curves, while the blue lines represent the first derivatives of the TG curves – DTG)

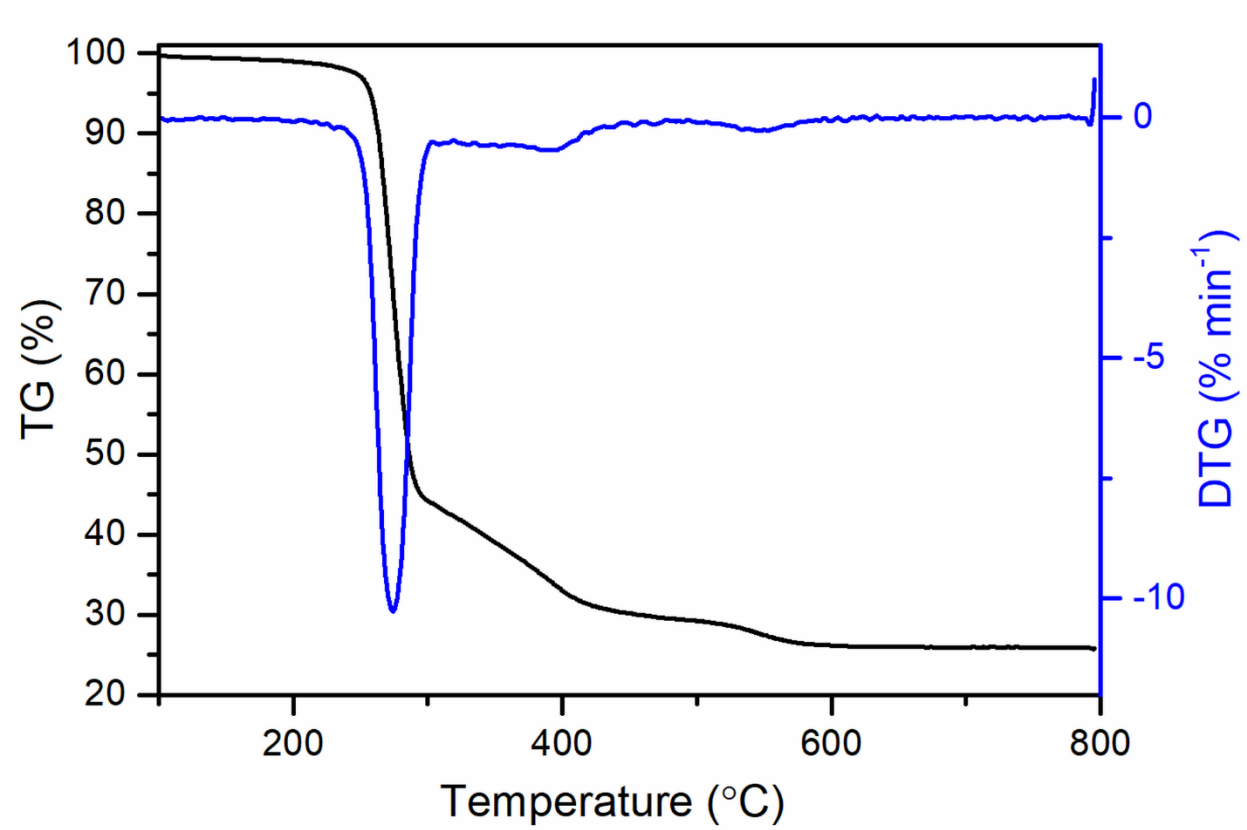

Figure S35. TG-DTG curve of the ***rac*-poly_3c_Ag** in a temperature range from 35°C to 300°C with a heating rate of 5°Cmin^{-1}(the black lines represent the TG curves, while the blue lines represent the first derivatives of the TG curves – DTG).

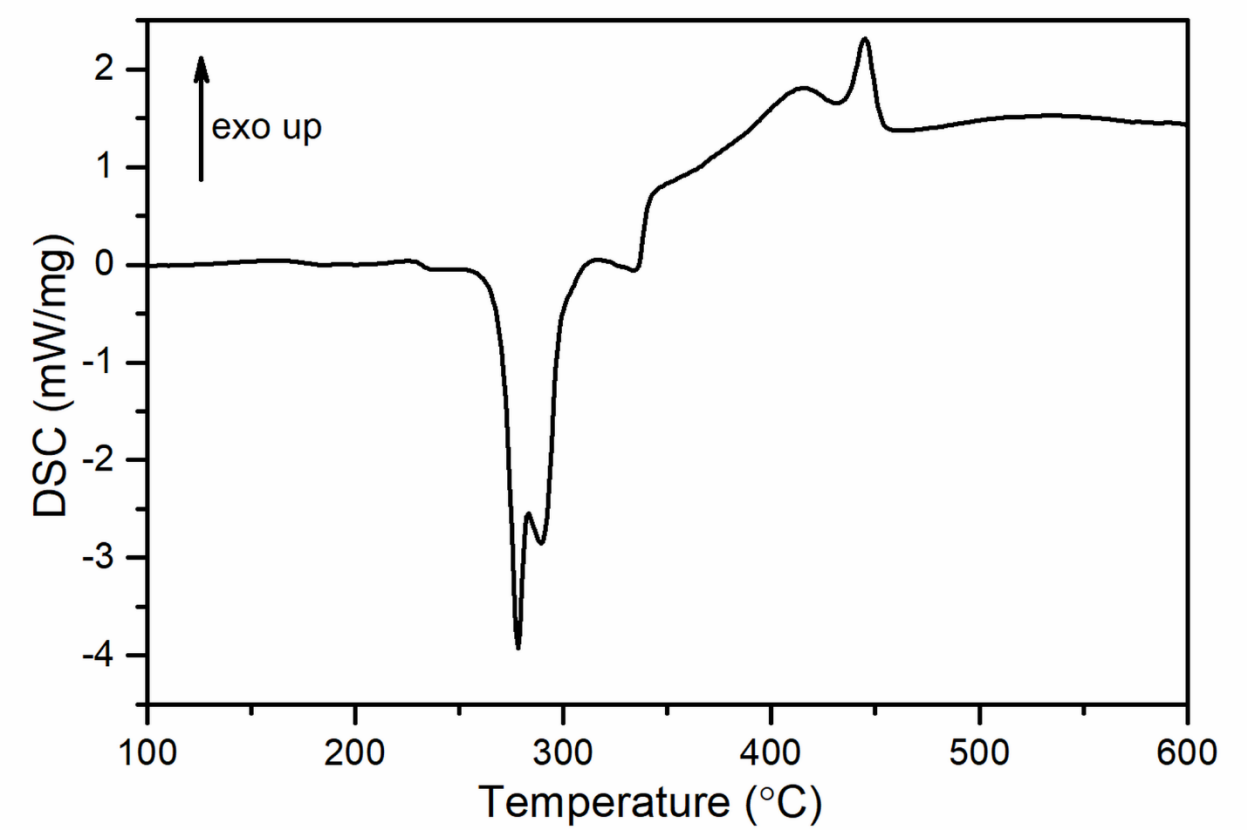

Figure S36. DSC curve of the ***rac*-poly_3a_Cu** in a temperature range from 35°C to 600°C with a heating rate of 10°Cmin^{-1}.

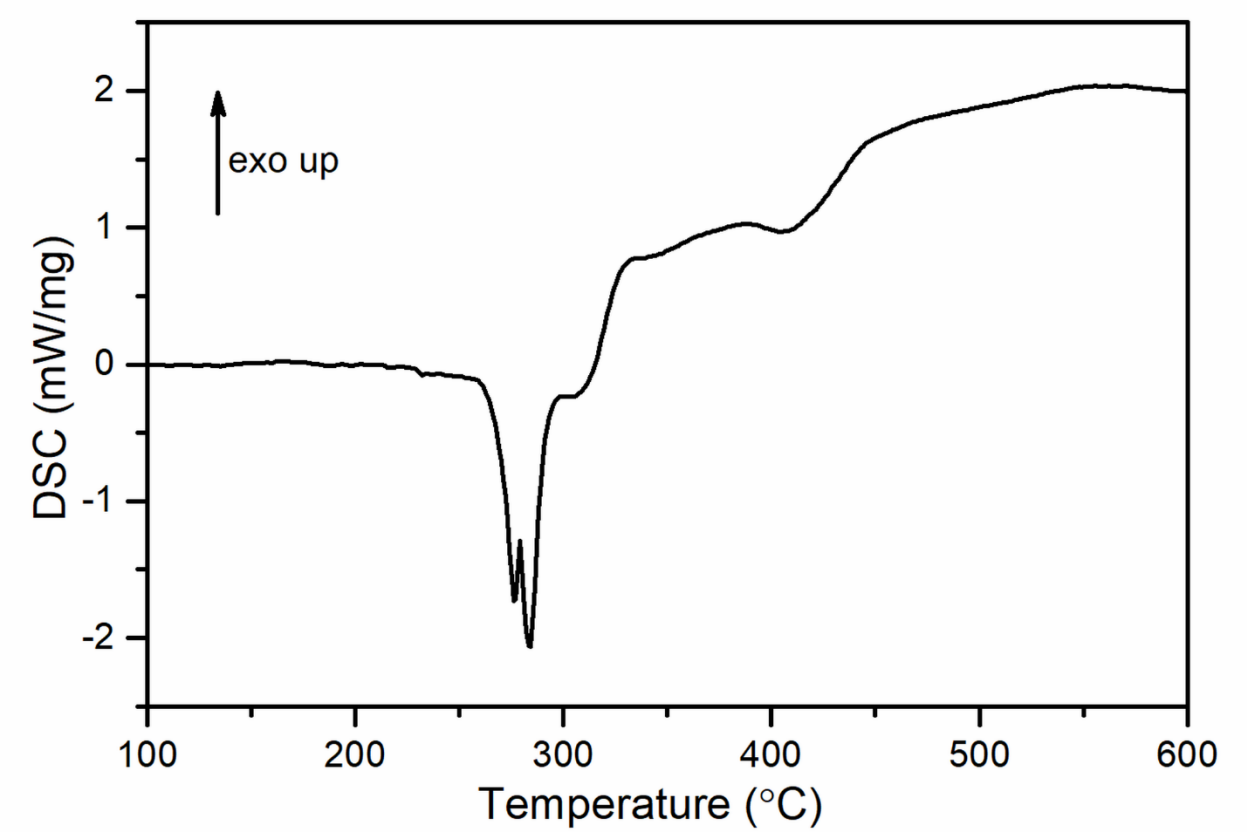

Figure S37. DSC curve of the ***rac*-poly_3c_Cu** in a temperature range from 35°C to 600°C with a heating rate of 10°Cmin^{-1}.

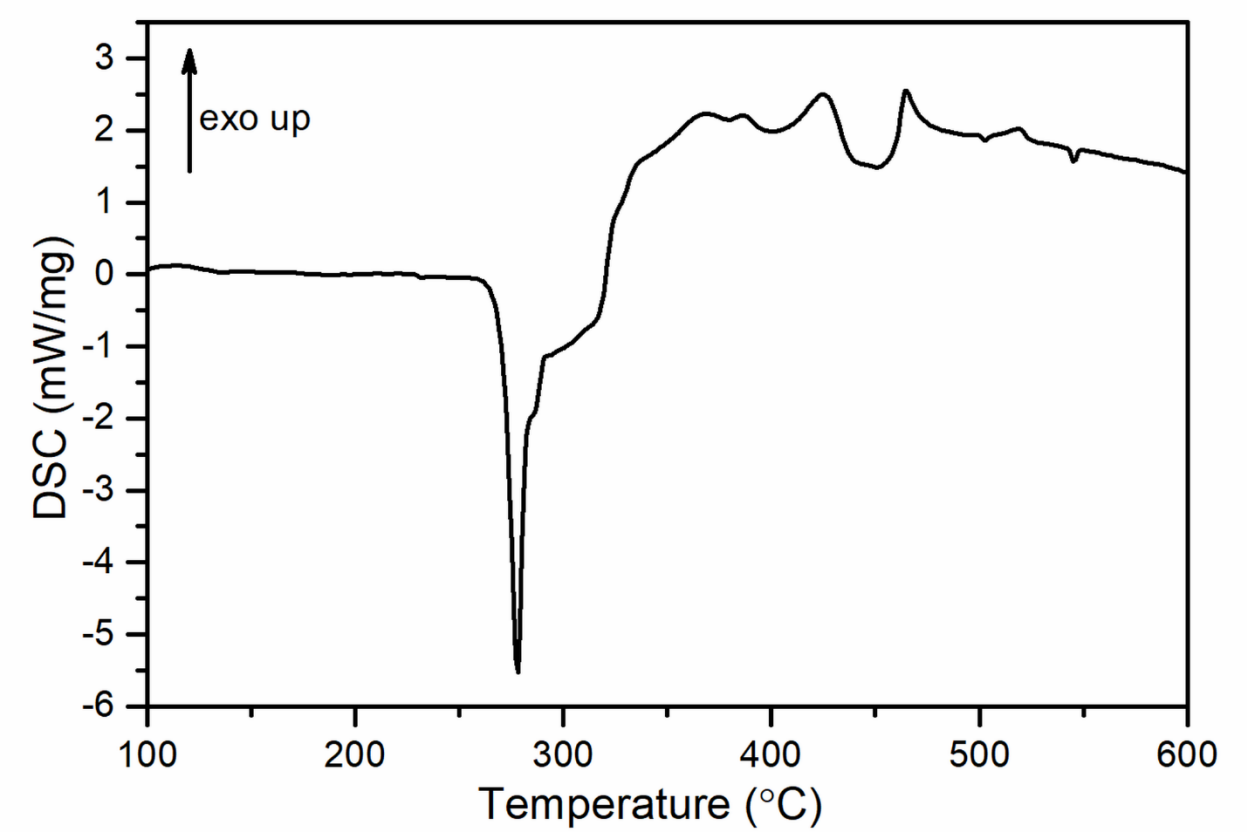

Figure S38. DSC curve of the ***meso*-poly_3a_Ag** in a temperature range from 35°C to 600°C with a heating rate of 10°Cmin^{-1}.

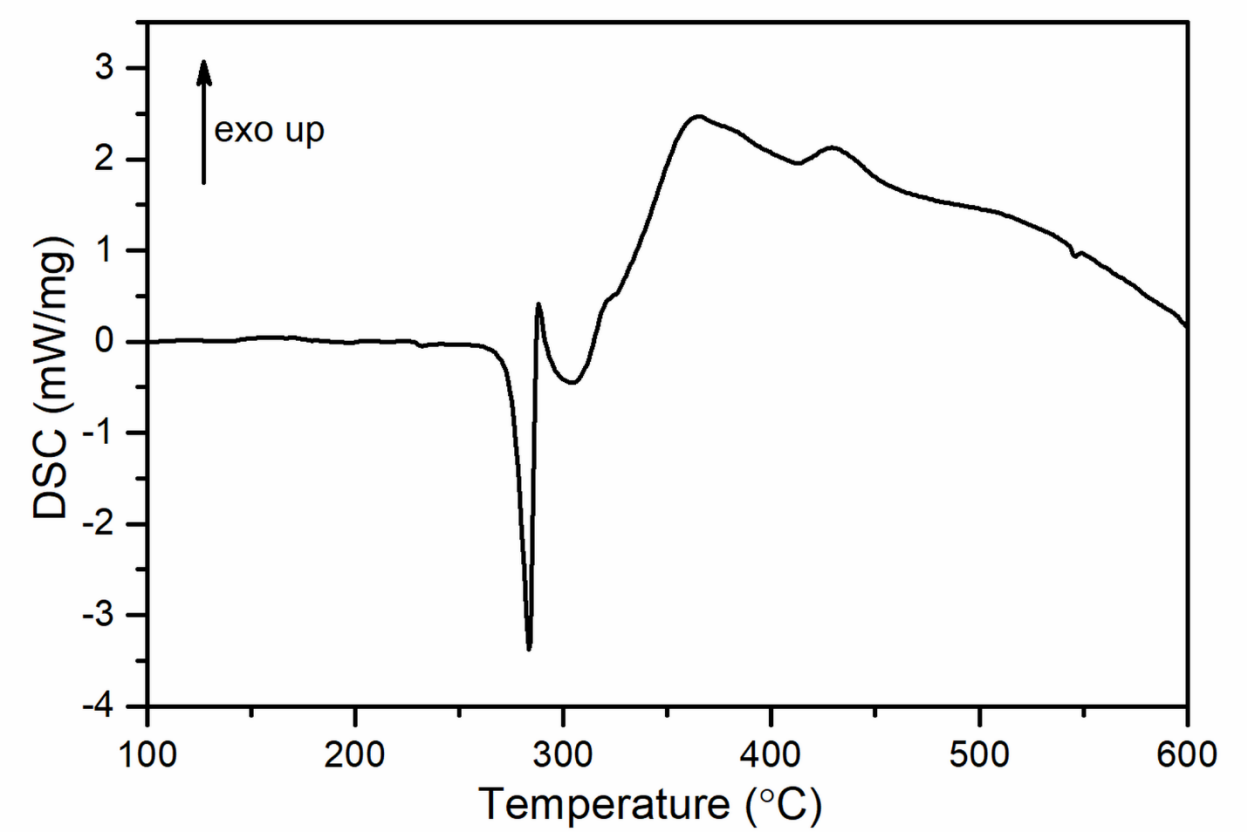

Figure S39. DSC curve of the ***rac*-poly_3c_Ag** in a temperature range from 35°C to 600°C with a heating rate of 10°Cmin^{-1}.

PART D. References

(1) Ziółkowska, A.; Szynkiewicz, N.; Ryl, J.; Ponikiewski, Ł. Group 11 complexes with a phosphanylphosphaalkene ligand: preparation and stability study. *Dalton Trans.* **2023**, *52* (15), 4658-4662.
(2) Sheldrick, G. A short history of SHELX. *Acta Crystallogr. A* **2008**, *64* (1), 112-122.
(3) Farrugia, L. WinGX and ORTEP for Windows: an update. *J. Appl. Cryst.* **2012**, *45* (4), 849-854.